



**OPTIMAL HARVESTING OF NILE PERCH, NILE TILAPIA, AND  
SMALL PELAGIC FISH POPULATIONS ON LAKE ALBERT, UGANDA**

**BY**

**GEOFFREY LUBANGAKENE**

**BSC. EDUC. (GULU)**

**2023/U/MSM/00781**


**A DISSERTATION SUBMITTED TO THE DIRECTORATE OF  
GRADUATE TRAINING, RESEARCH AND INNOVATIONS IN  
PARTIAL FULFILLMENT OF THE REQUIREMENTS LEADING TO  
THE AWARD OF THE DEGREE OF MASTER OF SCIENCE IN  
MATHEMATICS OF MUNI UNIVERSITY**

**November, 2025**

# Declaration

I, Geoffrey Lubangakene, hereby declare that this dissertation is a result of my original research work, and I present it without any reservations for external examination.

Name: ..... **Geoffrey Lubangakene** .....

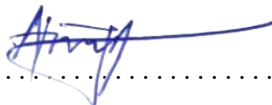
Signature: .....  ..... Date: ..... **09/11/2025** .....

# Approval

The research work culminating in this dissertation was conducted under my guidance and supervision.

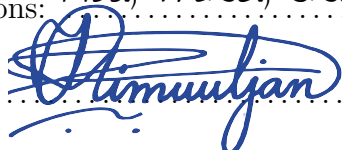
Name: Dr. Martin Deosborns Arop

Qualifications: PhD (Mak), MSc. (Mak), BSc. Educ. (GU)

Signature:  Date: 10/11/2025

Name: Dr. Kimuli Philly Ivan

Qualifications: PhD, MSc, BSc (Educ) - (Makerere)

Signature:  Date: 10th November 2025

# Dedication

This work is dedicated to my parents and my family. Your love and encouragement have always inspired me to strive for excellence. This work stands as a testament to your collective belief in me, and I am forever grateful.

# Acknowledgments

First and foremost, I give praise to the Almighty God who has made it possible for me to accomplish this work. I would like to express my appreciation to my supervisors, Dr. Martin Deosborns Arop and Dr. Kimuli Philly Ivan, for their guidance, commitment, and extreme patience throughout the writing of this dissertation. Their expertise and constructive feedback greatly shaped the direction and quality of this work.

Appreciation goes to Muni University for the opportunity to pursue a Master of Science in Mathematics and for providing a conducive learning environment. The knowledge and skills acquired during the program have been truly transformative. Special thanks to the staff of the Department of Mathematics for fostering a vibrant academic atmosphere and offering the resources essential for successful study.

I also extend heartfelt thanks to Gulu University, where I pursued my undergraduate studies in Bachelor of Science Education (Mathematics and Chemistry). The mentorship, knowledge, and academic environment that I experienced during my studies played a crucial role in preparing me for further studies. I am especially thankful for the dedicated lecturers and the opportunities for academic foundation that the University provided throughout my undergraduate journey.

My sincere appreciation goes to my former primary and secondary schools, Sir Samuel Baker School, Holy Rosary Primary School, and Lapainat Primary School, for their contributions to my early academic development. The dedicated teachers and supportive environment at each stage contributed significantly to shaping my academic character and instilling in me the values of hard work that have made me reach this far.

I would like to acknowledge the administration, teaching, and non-teaching staff of the Agung Community Secondary School, where I currently work. Your encouragement towards my further studies, moral support, and understanding shown throughout this academic journey are greatly appreciated.

I am equally grateful to the administration and teaching fraternity of Restore Leader-

ship High School, where I currently serve as a teacher in the mathematics department. That also generously offered me the opportunity to conduct my practicum and field engagement. The support from the administration, staff, and students created a conducive environment that aroused interest in further studies and strengthened my professional development.

Special thanks go to my classmates at Muni University for their mutual encouragement and collaboration throughout the coursework and research work. The support and friendship of Mr. Adiga Swadicki, Mrs. Ayiorwoth Pameala Mandawun (RIP), Mrs. Chandiru Zamuradi, Mr. Kiganga Samuel, Mr. Kituno Leo, Mr. Mazin Sadam, Mr. Onekgiu George, Mr. Omar Enima, Mr. Okello Moses, Mr. Taliban Jamal Baiti, and Mr. Tooki Raphael are gratefully acknowledged. Your friendly lifestyle made the academic journey both productive and enjoyable.

Deep gratitude is owed to friends whose inspiration, motivation, and belief provided constant encouragement. Appreciation goes to Dr. Walter Okongo, Mr. Akena Richard Otim, Mr. Bongomin Denis, Mr. Nyerogang Gabriel, Mr. Ocitti Innocent Bitali, Mr. Okello Billy, Mr. Okello Lawrence Oun, Mr. Okello Phillips, Mr. Okello Simon Peter, and all others, though unnamed here, whose support has left a meaningful impact on the success of my academic journey.

Most importantly, profound appreciation goes to my parents, Mr. Opoka Joseph and Mrs. Esther Aciro Opoka, whose unconditional love and guidance have shaped me into who I am today. I extend special thanks to my dear wife, Mrs. Brenda Sofi Lubangakene, whose boundless support and encouragement have been my strength throughout this journey. Appreciation to my beloved children, Edmond Omiya and Abigail Nimaro, your joy and laughter have been a constant reminder of the future that I am working toward. Sincere thanks to my brothers and sisters, Lilian Atoo, Joyce Adokorach, Milly Aloyo Opoka, Brenda Rachael Alaroker, Daniel Mic Pa Lacwec, Oscar Olal, Eunice Adong, Bosco Oryem, and Brenda Abalo. Your constant love and encouragement have always inspired me to strive for excellence. I am deeply grateful for your support and for always being by my side.

# Table of Contents

<b>Declaration</b>	<b>i</b>
<b>Approval</b>	<b>ii</b>
<b>Dedication</b>	<b>iii</b>
<b>Acknowledgment</b>	<b>iv</b>
<b>List of Figures</b>	<b>ix</b>
<b>List of Tables</b>	<b>x</b>
<b>Acronyms and Abbreviations</b>	<b>xi</b>
<b>Abstract</b>	<b>xii</b>
<b>1 Introduction</b>	<b>1</b>
1.1 Background . . . . .	1
1.2 Statement of the Problem . . . . .	4
1.3 Objectives of the Study . . . . .	4
1.3.1 Main objective . . . . .	4
1.3.2 Specific objectives . . . . .	4
1.4 Scope of the Study . . . . .	4
1.5 Materials and Methods . . . . .	5
1.5.1 Establishing the optimal harvesting strategies for fish populations under a constant yield harvesting model . . . . .	5
1.5.2 Ascertaining the optimal conditions for the co-existence of fish pop- ulations under a constant effort harvesting model . . . . .	6
1.6 Significance of the Study . . . . .	6
1.7 Organisation of the Dissertation . . . . .	6
<b>2 Literature Review</b>	<b>8</b>
2.1 Fish Harvesting Models . . . . .	8

2.2	Optimal Fish Harvesting Models . . . . .	10
<b>3</b>	<b>The Optimal Harvesting Strategies for Fish Populations under Constant Yield Harvesting Model</b>	<b>13</b>
3.1	Introduction . . . . .	13
3.2	Model Formulation . . . . .	13
3.2.1	Definitions of variables and parameters . . . . .	14
3.2.2	Model assumptions . . . . .	14
3.2.3	Compartmental diagram . . . . .	14
3.2.4	The state equations . . . . .	15
3.3	Existence and Uniqueness of State Solutions . . . . .	16
3.4	Existence and Uniqueness of the Optimal Controls . . . . .	18
3.5	Positivity and Boundedness of the State Solutions . . . . .	18
3.6	The Optimality System . . . . .	21
3.6.1	Adjoint equations . . . . .	21
3.6.2	Optimality condition . . . . .	21
3.7	Parameter Estimation . . . . .	25
3.8	Numerical Simulations . . . . .	26
3.8.1	Optimal solutions . . . . .	27
3.8.2	Dynamics of fish populations with different harvest rates . . . . .	28
3.8.3	The influence of different initial biomass on the dynamics of fish populations . . . . .	29
<b>4</b>	<b>The Optimal Conditions for the Co-existence of Fish Populations under Constant Effort Harvesting Model</b>	<b>31</b>
4.1	Introduction . . . . .	31
4.2	Model Formulation . . . . .	31
4.2.1	Definitions of variables and parameters . . . . .	31
4.2.2	Model assumptions . . . . .	32
4.2.3	Compartmental diagram . . . . .	32
4.2.4	The state equations . . . . .	33
4.3	Existence and Uniqueness of State Solutions . . . . .	34
4.4	Existence and Uniqueness of the Optimal Controls . . . . .	35
4.5	Positivity and Boundedness of the State Solutions . . . . .	35
4.6	The Optimality System . . . . .	36
4.6.1	Adjoint equations . . . . .	36
4.6.2	Optimality condition . . . . .	37
4.7	Parameter Estimation . . . . .	40
4.8	Numerical Simulations . . . . .	41

4.8.1	Optimal solutions . . . . .	42
4.8.2	Dynamics of fish populations with different harvest rates . . . . .	43
4.8.3	The influence of different initial biomass on the dynamics of fish populations . . . . .	44
<b>5</b>	<b>Discussions, Conclusions, and Recommendations</b>	<b>46</b>
5.1	Introduction . . . . .	46
5.2	Discussions . . . . .	46
5.3	Conclusions . . . . .	48
5.4	Recommendations . . . . .	49
	<b>References</b>	<b>50</b>
	<b>Appendices</b>	<b>53</b>
	Appendix A: Definition . . . . .	53
	Appendix B: MATLAB codes for solving the model under constant yield harvesting	54
	Appendix C: MATLAB codes for solving the model under constant effort harvesting . . . . .	59

# List of Figures

3.1	The compartmental diagram for the food chain model. . . . .	15
3.2	(a) Optimal harvest rate and (b) Biomass of small pelagic fish, Nile tilapia, and Nile perch under constant yield harvesting strategies. . . . .	27
3.3	Variation of fish populations with time for different harvest rates: (a) small pelagic fish, (b) Nile tilapia, (c) Nile perch . . . . .	29
3.4	Variation of fish populations with time for different initial conditions ( $2 \leq (N_i)_0 \leq 30 \quad i = 1, 2, 3$ ) . . . . .	30
4.1	The compartmental diagram for the food chain model. . . . .	33
4.2	(a) Optimal harvest rate and (b) Biomass of small pelagic fish, Nile tilapia, and Nile perch under constant effort harvesting strategies. . . . .	42
4.3	Variation of fish populations with time for different harvest rates: (a) small pelagic fish, (b) Nile tilapia, (c) Nile perch . . . . .	44
4.4	Variation of fish populations with time for different initial conditions ( $2 \leq (N_i)_0 \leq 30 \quad i = 1, 2, 3$ ) . . . . .	45

# List of Tables

3.1	Parameter descriptions and values under constant yield harvesting strategies.	26
3.2	Summary of the results for the optimal solutions under constant yield harvesting strategies. . . . .	28
4.1	Parameter descriptions and values under constant effort harvesting strategies.	41
4.2	Summary of the results for the optimal solutions under constant effort harvesting strategies. . . . .	43

# Acronyms and Abbreviations

<b>FBS</b>	Forward-backward sweep
<b>ODE</b>	Ordinary Differential Equation
<b>PMP</b>	Pontryagin's maximum principle
<b>RK4</b>	Fourth-order Runge-Kutta
<b>SDGs</b>	Sustainable Development Goals

# Abstract

In this dissertation, an optimal fish harvesting problem for harvesting small pelagic fish, Nile tilapia, and Nile perch within a food chain, modelled with constant yield and constant effort harvesting, is considered. In particular, the optimal harvesting strategy that ensures both economic benefits and ecological sustainability of fish species was determined. The models were based on nonlinear ordinary differential equations that account for logistic growth, harvest, and species interactions. The problem is motivated by the need to address the concern of decreasing fish populations, resulting from overfishing and unsustainable harvesting practices.

The optimality system, comprising the state equations, adjoint equations, and optimality condition, was derived using Pontryagin's maximum principle. A forward-backward sweep method based on fourth-order Runge–Kutta schemes was employed to solve the optimality system. Peano's existence theorem and Lipschitz uniqueness theorem were used to prove the existence and uniqueness, respectively, of solutions to the state equations.

Numerical results show that for constant yield harvesting, harvest rates remained constant throughout the simulation period, with the highest harvest rate recorded for Nile perch and the lowest for Nile tilapia. In contrast, under constant effort harvesting, the highest harvest rate is again recorded for Nile perch, while the lowest is for small pelagic fish. Constant effort harvesting strategies allow fish populations to adjust dynamically and support ecological resilience. Whereas, constant yield harvesting risks overexploitation with any slight increase in harvest rates above the optimal level.

The study recommends optimal harvesting strategies for Lake Albert, Uganda, as they promote ecological sustainability by preventing both overexploitation and underutilisation of resources. Fisheries managers should maintain fish populations at a moderate level by enforcing zero harvests when fish biomass is low to ensure faster recovery and reduce the risk of species extinction.

# Chapter 1

## Introduction

### 1.1 Background

The problem of optimal fish harvesting involves determining optimal harvesting strategies that enhance both ecological sustainability and the long-term economic benefits of fisheries. Consequently, various harvesting strategies can be incorporated into the model, for example, constant yield, constant effort, periodic, proportional threshold, and rotational strategy (Alfred, 2016; Idels & Wang, 2008; Laham et al., 2012). This study considered constant yield and constant effort harvesting strategies due to their simplicity and practical relevance to fisheries management, as they closely reflect real-world practices where authorities regulate catches through fixed quotas or maintain stable fishing effort levels. Optimal control problems are applied broadly in diverse fields of biological sciences, economics, physics, computer science, and engineering, for example, in biological modelling, ecosystem management, taxation, and vibration control (Anița et al., 2011; Chen & Islam, 2005; La Torre et al., 2015; Lenhart & Workman, 2007).

The dynamics of fish population can be described using the system of ordinary differential equations, discrete equations, partial differential equations, stochastic differential equations, integro-difference equations, or a combination of these equations (Lenhart & Workman, 2007). In this study, ordinary differential equations are used to determine optimal control strategies to harvest Nile perch (*Lates niloticus*), Nile tilapia (*Oreochromis niloticus*), and small pelagic fish (*Neobola bredoi*). The temporal dynamics of fish populations are continuous and are best modelled by the ODE system. This system is used in the long-term evaluation of the trend of fish populations under a given harvesting strategy (Mpele et al., 2014a).

Optimal control problems for fish harvesting help ensure the sustainability of fish stocks, economic stability in the fishing industry, and the preservation of the ecosystem (Seijo et al., 1998). However, overfishing caused by poor management and overexploitation of

fish populations can result in the collapse of fish stocks, lowering the diverse benefits of fishing (Rossi, 2022). Fisheries managers can use dynamic optimisation frameworks and bio-economic models to establish optimal fish harvesting. This is crucial for managing fish resources to achieve long-term benefits and prevent overexploitation (Da Rocha et al., 2012). This study focuses on constant yield and constant effort harvesting strategies. Constant yield harvesting is where a fixed amount of fish stock is harvested from the population within a given period, without considering the available fish population. However, constant effort harvesting involves adjusting the harvest rate, which depends on the population size (Alfred, 2016; Idels & Wang, 2008; Maurya & Priyadarshi, 2020).

Fish harvesting is vital for local communities and the global economy, supporting food security and livelihoods, particularly in developing regions like Africa. Small-scale fish harvesting supports food security and livelihoods by providing essential proteins and nutrients to people worldwide (McDougall, 2023). On a larger scale, industrial fish harvesting contributes significantly to the global economy. As stated by Béné et al. (2015), 15% of the animal protein consumed per person comes from fish, feeding more than 4.5 billion people around the world, making it the main source of revenue and indirect food security. However, long-term monitoring of fish stocks indicates that the condition of fishery resources has been steadily declining. The percentage of fish stocks that are within ecologically viable limits decreased from 90% to 65.8% between 1974 and 2017 (Action, 2020).

Progress in fisheries management underscored the connection between fishing effort, mortality, and fish stock dynamics, laying the foundation for key concepts such as maximum sustainable yield for policy benchmarking and the identification of overfishing. As evidence of overfishing increased in the 1960s, fisheries faced difficulties in enforcing control due to imperfect property rights, leading to voluntary harvest restrictions (Wilén, 2000). The publication of Pontryagin's work in 1962 on optimal control theory (Pontryagin et al., 1962) boosted the natural resource economics on the conceptual core of resource dynamic analysis. By the end of the 1960s, the techniques were applied to optimising both renewable and nonrenewable resources, shaping modern fisheries management strategies. Without optimal fish harvesting, the fisheries are vulnerable to depletion, which has negative economic and ecological effects (Clark and Munro, 1975). These optimal control problems employ mathematical and computational models to find optimal harvest rates that prevent overexploitation and ensure the long-term success of fisheries. The objective is to determine the optimal harvest rate that maintains the productivity of fish populations for a long period (Clark, 1990). These models have become key approaches in fisheries management that offer guidelines for sustainable yield that maintain fish stocks for future generations.

Despite advances in optimal fish harvesting problems, computational challenges persist due to the complexity of fish population dynamics, environmental changes, inter-species interaction, variable harvesting pressures, and limited data (Kellner & Sweeney, 2016). Numerical solutions are essential for solving these models, but face challenges such as high processing costs, computational intensity, and sensitivity to initial and boundary conditions (Hannachi & Hossain, 2017). Therefore, careful implementation and validation are necessary to ensure that the results are reliable and applicable to actual fisheries management.

Several models have been extensively studied to determine the optimal fish harvesting strategies using ordinary differential equations as follows. To start with, Clark and Munro (1975) presented the optimal control problem for the dynamics of the fisheries economics model, using constant effort harvesting under linear and nonlinear control frameworks. Their model considered logistic terms and harvest terms for a single fish species, excluding predator-prey relations within the ecosystem, which are critical for understanding multi-species fisheries.

In related work, Chaudhuri (1986) extended the application of optimal control theory to multi-species fish populations. The model accounted for logistic growth and interaction terms due to the competition between two species of fish for the use of common resources, but not for the impact of predator-prey interaction. In addition, Khamis et al. (2011) presented optimal harvest strategies for one predator and two species of prey fish. Two homogeneous patches of the free fishing zone and the no-fishing zone were considered, incorporating immigration of the prey species between the two zones with and without a predator. However, only one species of prey fish was subjected to constant effort harvesting.

Further developments in fisheries models include the work by Mpele et al. (2014a) who proposed an optimal control problem in a three-species fisheries system interacting in a predator-prey manner. They studied the optimal taxation strategy, in which all species were subjected to constant effort harvesting. In addition, Sahoo and Poria (2015) developed an optimal control problem for a prey-predator model of three species, with the primary goal of studying the effects of providing allochthonous input to the super predator. But the model only subjected the super predator to harvest.

Furthermore, Demir and Lenhart (2019) developed a three-level food chain model for black sea anchovy, zooplankton, and jellyfish. However, only the anchovy fish species was subjected to constant effort to incorporate seasonal harvest. In this study, the work

presented by [Demir and Lenhart \(2019\)](#) is extended to the optimal control problem of harvesting three species of fish: small pelagic fish, Nile tilapia, and Nile perch, but using constant yield and constant effort harvesting strategies.

## 1.2 Statement of the Problem

The challenge of optimal fish harvesting lies in balancing economic benefits, ecological sustainability, and preservation of fish populations. Parts of this challenge have been addressed in previous studies: [Demir and Lenhart \(2019\)](#) studied constant effort harvesting within a three-species food web for black sea anchovy, zooplankton, and jellyfish, but applied it to only the anchovy fish species. [Mpele et al. \(2014a\)](#) studied the population dynamics of small pelagic silver fish, Nile perch, and Nile tilapia under constant effort harvesting with taxation as a control, but did not consider a constant yield approach. Unfortunately, none of those works involve both constant yield and constant effort models across all three fish species. This study establishes an optimal harvesting problem that applies both constant yield and constant effort to small pelagic fish, Nile tilapia, and Nile perch.

## 1.3 Objectives of the Study

### 1.3.1 Main objective

To determine optimal harvesting strategies for Nile perch, Nile tilapia, and small pelagic fish populations using both constant yield and constant effort harvesting models.

### 1.3.2 Specific objectives

- (a) To establish optimal harvesting strategies for fish populations under a constant yield harvesting model.
- (b) To ascertain the optimal conditions for the co-existence of fish populations under a constant effort harvesting model.

## 1.4 Scope of the Study

This study focuses on optimal fish harvesting for the dynamics of three fish species within a food chain consisting of small pelagic fish, Nile tilapia, and Nile perch. The study is

restricted to ordinary differential equations to analyse the dynamics of fish populations over time. The model considered both constant yield and constant effort harvesting.

The study is limited to the ecosystem of Lake Albert, Uganda. Although the study centered on Lake Albert, the framework can be applied to similar aquatic environments where fishery management is crucial. The study also analyses the dynamics of the short-term and long-term population of fish and the impacts of harvesting strategies. Pontryagin's maximum principle was used in deriving the optimality system, which consisted of the state equations, the adjoint equations, and the optimality condition. The optimality system was approximated using the forward-backward sweep method. The fourth-order Runge-Kutta method was employed to determine the solutions of the state equations and adjoint equations. Peano's existence theorem and Lipschitz uniqueness theorem were applied in proving the existence and uniqueness, respectively, of the solutions to the ODE system. The study was carried out over a period of one academic year.

## 1.5 Materials and Methods

The following materials and methods are employed to achieve the objectives set out in the study.

### 1.5.1 Establishing the optimal harvesting strategies for fish populations under a constant yield harvesting model

The dynamics of fish populations were formulated as a system of nonlinear ordinary differential equations of the form

$$\frac{dx}{dt} = f(t, x, h), \quad x(0) = x_0, \quad (1.1)$$

where  $x(t)$  represents the fish population and  $h(t)$  denotes the constant yield harvesting rate. The existence of the state solution was established using Peano's Existence Theorem, provided  $f(t, x, h)$  is continuous. The Lipschitz Uniqueness Theorem was used to prove the uniqueness of the state solution, on the condition that  $f(t, x, h)$  satisfies the Lipschitz condition. Pontryagin's maximum principle was employed to derive the optimality system of the optimal control problem. Then the forward-backward sweep method was used to approximate the solutions of the optimality system. The fourth-order Runge-Kutta method was employed to solve the optimality system. MATLAB (R2023a) software was employed to perform numerical simulations and analyse the long-term behavior of the fishery model using a computer equipped with an Intel Core i3 processor, 16 GB RAM, and a 64-bit Windows 11 operating system.

### 1.5.2 Ascertaining the optimal conditions for the co-existence of fish populations under a constant effort harvesting model

The fish population dynamics were formulated using a system of nonlinear ODEs as expressed in (1.1), with  $h(t)$  denoting the constant effort harvesting rate. Peano's Existence Theorem was used to prove the existence of the state solution provided that  $f(t, x, h)$  is continuous. The Lipschitz uniqueness theorem was applied to guarantee the uniqueness of the state solutions of the state system (1.1), given  $f(t, x, h)$  satisfies the Lipschitz condition. To derive the optimality system of the optimal control problem, Pontryagin's maximum principle was used. Then, the forward-backward sweep method was used to approximate the solutions of the optimality system. The fourth-order Runge-Kutta method was employed to solve the optimality system. MATLAB software was used to perform numerical simulations and analyse the long-term behavior of the fishery model on a 64-bit Windows 11 computer with an Intel Core i3 processor and 16 GB RAM.

## 1.6 Significance of the Study

In this study, the primary aim is to promote sustainable fishery management by employing optimal fish harvesting strategies, specifically constant yield and constant effort harvesting. This work focuses on the three key species of fish in Lake Albert: small pelagic fish, Nile tilapia, and Nile perch. This study is significant for communities that depend on fisheries as a vital source of food security, income, and employment. By determining optimal fish harvesting strategies, the research contributes to economic stability and sustainable food supplies, without compromising the future productivity of the resources. The results of this research align with and support the achievement of the Sustainable Development Goals (SDGs), particularly SDG 1, No Poverty, and SDG 2, Zero Hunger, by improving food security and sustainable livelihoods.

## 1.7 Organisation of the Dissertation

This dissertation consists of five chapters. In this Chapter 1, an introduction to the study, outlining the background of the study, statement of the problem, the objectives of the study, the scope, the method and materials used to show how the specific objectives were achieved, and the significance of the study. A comprehensive review of the literature on mathematical models for fish harvesting and on optimal fish harvesting problems under different harvesting strategies modelled with ordinary differential equations is discussed in Chapter 2. In Chapter 3, the formulation of the mathematical model, and both theoretical and numerical analysis under constant yield harvesting strategies are presented. In

Chapter 4, the mathematical formulation of the models under constant effort harvesting strategies is discussed, together with theoretical and numerical analysis. In Chapter 5, discussions, conclusive remarks, and recommendations for further research are given.

# Chapter 2

## Literature Review

In this chapter, literature on mathematical models for fish harvesting is reviewed, along with studies on optimal fish harvesting problems under different harvesting strategies modelled with ordinary differential equations.

### 2.1 Fish Harvesting Models

Studies on the system of ordinary differential equations for fish harvesting using various harvesting techniques, which are not optimal control problems, are presented as follows.

Idels and Wang (2008) developed a mathematical model for fisheries management with different fish harvesting strategies. They used an ODE model for a single species, which incorporates logistic growth and harvest terms under constant yield, proportional, seasonal, proportional threshold, and rotational harvesting strategies. The study aimed to determine the impact of different fish harvesting strategies on equilibrium values. Qualitative analysis and numerical simulations were performed using numerical methods to determine the impact of the five fish harvesting strategies. Their findings showed that the equilibrium values and the rate at which the population attains equilibrium change depending on the harvest term. Their study overlooked the impact of other species within the same ecosystem by focusing on the fisheries management of a single species. In this study, the model included three species, taking into account the impact of the logistic growth term, prey-predator interaction, and harvest term under constant effort and constant yield harvesting strategies.

Additionally, logistic growth models for management of fish harvesting strategies were presented by [Laham et al. \(2012\)](#). They studied tilapia fish harvesting strategies using two models of logistic growth terms, subject to constant yield harvesting and seasonal harvesting. The objectives of their study were to compare the different results obtained

from the two strategies and to determine the maximum harvest amount that could maintain a continuous supply of tilapia fish. Numerical methods were used in the numerical simulations. The results showed that the best harvesting strategy is the logistic seasonal harvesting strategy since it can improve productivity. Using logistic constant yield harvesting removes a fixed quantity of fish regardless of stock size, which does not give sufficient time for the fish population to recover, leading to a high risk of unsustainable fishing. They considered a single fish species in the ODE for logistic growth models using constant yield harvesting and seasonal harvesting, but not constant effort harvesting. The model also excluded the predator-prey interaction within the ecosystem. In this study, an optimal fish harvesting model was used for three species of fish that interact in a predator-prey manner, applying constant yield and constant effort harvesting.

Another mathematical model for maximum fish harvesting was studied by [Alfred \(2016\)](#) employing constant yield, constant effort, and periodical harvesting strategies to prevent the extinction of the wrasse fish population. They formulated three ODE models of logistic growth terms under different harvesting strategies. The objective of the study was to determine the maximum growth and reproduction of the wrasse fish species. Numerical methods were applied to analyse and visualise the changes in fish biomass over time for all harvesting strategies. The result revealed that constant yield harvesting does not give enough time for fish to recover if it exceeds the bifurcation point. However, constant effort harvesting could also drive the fish population to extinction if the harvesting rate surpasses the bifurcation point or the population's growth rate. However, the model considered only a single fish species, leaving out other species in the ecosystem that constitute the structure of the food web. In contrast, this study incorporates three species in the food chain model using constant yield and constant effort harvesting strategies.

In addition, [Raymond et al. \(2019\)](#) proposed a model of predator-prey fishery, with constant effort harvesting incorporated into all fish populations. They modelled the ecological dynamics of a predator and two-prey system of fishery using three nonlinear autonomous ODEs following the Holling type II function response. They aimed to analyse the effect of fish harvesting on both prey and predator populations. Local stability condition was obtained using the Routh-Hurwitz Criterion method and eigenvalue approach. By specifying the appropriate Lyapunov function, the coexistence equilibrium point was proved for global stability. The model was numerically simulated using MATLAB's ODE solvers. Both the numerical and analytical findings showed that the three fish species would coexist when the two prey species were not overharvested beyond their intrinsic growth rates. This is because prey populations contribute highly to the growth rates of the predator population. The model only incorporated constant effort harvesting strategies. In this study, optimal fish harvesting models are used, as they provide a

mathematical foundation to balance both ecological sustainability and economic benefits.

## 2.2 Optimal Fish Harvesting Models

The following review of the literature is limited to optimal fish harvesting problems under different harvesting strategies and focuses on applying optimal control theory to systems governed by ordinary differential equations.

[Clark and Munro \(1975\)](#) used the optimal control theory to study the dynamics of the fisheries economic model. The logistic equation of population dynamics with a constant effort harvesting rate served as the basis for the ODE model for a single fish species. They did not consider predator-prey interaction within the ecosystem. Their objective was to maximise the current value of fish yield for both linear and nonlinear control problems. Using Pontryagin's maximum principle, the necessary conditions for optimality were derived in both situations. The optimal control variable in terms of state and adjoint variable was determined by solving the maximised Hamiltonian using the implicit function theorem for nonlinear optimal control problems. In contrast, a Bang-Bang feedback control law governed the solution for linear optimal control problems. Their result showed that fisheries economics can easily be framed within a capital-theoretic framework with the help of optimal control theory, producing outcomes that are both broadly applicable and easily understood. An Optimal control problem that includes harvesting three species of fish that interact in a predator-prey manner was considered in this study.

Also, a bioeconomic ODE model was studied by [Chaudhuri \(1986\)](#) for harvesting a multispecies fishery following logistic growth, with combined harvesting effort for both competing fish species. The study's objective was to analyse the economic implications of optimal fish harvesting strategies with joint harvesting of two competing fish species. Pontryagin's maximum principle was used in the formulation of the optimal solution. The RK4 method was used to determine the optimal solution. The result showed that a fishery can attain bioeconomic stability as well as dynamic stability when the coefficients of interspecific competition are less than those of their coefficients of intraspecific competition. The model incorporated logistic growth and interaction terms because of competition between two fish species for the use of common resources, but not for the impact of predator-prey interaction. This model extends to three fish species interacting in a predator-prey manner with different harvesting rates for each species, using constant effort and constant yield harvesting.

Additionally, the optimal harvesting strategies for one predator and two prey fish species

using an ordinary differential equation were presented by [Khamis et al. \(2011\)](#). They studied the dynamics of the fishery in the two homogeneous patches of free fishing zone and no-fishing zone, incorporating immigration of the prey species between the two zones with and without predators. However, only one prey fish species was subjected to constant effort harvesting. Their objective was to select the harvesting method that maximises the net profit gained from selling the fish. Using Pontryagin's maximum principle, the necessary conditions for optimality were determined. The RK4 method was used to solve the optimality system. The optimal control was a combination of the singular control and the Bang-Bang, since the problem was a linear optimal control. It was discovered that the fish populations are less sensitive to the catchability coefficient but more sensitive to predation rates, growth, and dispersal. This study considered the harvest of all three species of fish with constant effort and constant yield harvesting.

Another study on optimal taxation strategies in a three-species fishery system was investigated by [Mpele et al. \(2014a\)](#), where the species interacted in a predator-prey manner, with all species subjected to constant effort harvesting. To control fishing efforts, they proposed a bioeconomic mathematical model based on Lotka-Volterra dynamics, and taxation on the profit per unit biomass of harvested fish was used as a control variable. The optimality condition was determined using Pontryagin's maximum principle, and the FBS scheme implemented by the RK4 method was used to solve the optimal solution. Numerical results indicate that optimal taxation ensures sustainable fishing efforts and species conservation. However, tax policies are effective tools for fishery management; the result showed that low taxes can lead to overfishing and species extinction, while high taxes reduce fishing efforts, leading to overabundant fish populations. Hence, bioeconomic balance is achieved at optimal tax rates and harvesting effort levels to maximise total discounted net revenue. The model did not include constant yield harvesting as one of the harvesting strategies and only included linear cost terms in the cost functional, which would exclude additional costs associated with the interference between vessels and their workers from the model. In this study, a nonlinear optimal control problem for fish harvesting was formulated using constant yield and constant effort harvesting.

Furthermore, [Sahoo and Poria \(2015\)](#) developed an optimal control problem for a three-species prey-predator ODE model, which provided allochthonous inputs to the super predator following the Holling type II function response with the super predator subjected to constant effort harvesting. Their primary goal was to study the effects of providing allochthonous inputs to the super predator population while incorporating constant effort harvesting strategies. Pontryagin's maximum principle was used to characterise the optimal control with fishing effort used as a control variable. The optimal control problem was solved numerically using the forward-backward sweep technique of the fourth-order

Runge-Kutta method to investigate the numerical simulations. According to their findings, the danger of extinction of the top predator decreases as allochthonous resources become more accessible in the presence of harvesting. Their model had only subjected the super predator to harvesting. This study included optimal harvesting of small pelagic fish, Nile tilapia, and Nile perch with constant yield and constant effort harvesting strategies.

According to [Demir and Lenhart \(2019\)](#), food chain models with interactions between key species are useful tools for ecological conservation and economic sustainability in commercial fisheries. They studied the optimal sustainable fishery management of the Black Sea anchovy with the food chain model using constant effort harvesting, incorporating seasonal harvesting. They considered three trophic levels that represent the food web dynamics between Black Sea anchovy, jellyfish, and zooplankton. Their study only considered the harvest of one fish species. Their main aim was to find the optimal harvesting strategy for the discounted net profit value of the anchovy fishery, which offers a sustainable anchovy fishery. The necessary conditions satisfying an optimal control and their corresponding states were derived using Pontryagin's maximum principle. The fourth-order Runge-Kutta method was used to solve the optimality system, and the forward-backward sweep method was used to approximate the solutions of the optimality system. For parameter estimation, the ordinary least squares method was used. When the harvesting strategies were compared, it was discovered that the optimal harvest strategy yields 44% more net profits than the current strategy. In this study, both constant yield and constant effort harvesting were applied to all three fish species.

Turning to the present study, the work of [Demir and Lenhart \(2019\)](#) is extended to a food chain consisting of small pelagic fish, Nile tilapia, and Nile perch. The aim is to establish the optimal harvesting strategies for fish populations using constant yield and constant effort harvesting models. In particular, ordinary differential equations (ODEs) were used to formulate the dynamics of fish populations, where all three fish species are subjected to harvesting.

# Chapter 3

## The Optimal Harvesting Strategies for Fish Populations under Constant Yield Harvesting Model

### 3.1 Introduction

In this chapter, the model formulation that incorporates constant yield harvesting is presented. This is followed by a theoretical investigation of the existence and uniqueness of the state and control variables. Furthermore, the positivity and boundedness of the state solutions are analysed to ensure that the model is biologically feasible. In addition, the optimality system was derived to establish the state equation, adjoint equation, and optimality condition. Next, approximation with the fourth-order Runge-Kutta method and parameter estimations are presented. Finally, numerical simulations were performed to find the optimal solutions and the dynamics of fish populations with different harvest rates.

### 3.2 Model Formulation

This section presents the optimal harvesting problem with non-linear ODEs. Optimal harvest strategies are determined for fish species, all of which are subjected to constant yield harvesting. Three trophic levels were used to represent the behavior of the food web system, which consists of small pelagic fish, Nile tilapia, and Nile perch. The layout of this section is the definitions of variables and parameters. This is followed by the assumptions of the model and the compartmental diagram for the food chain. Lastly, the state equations and the cost functional were formulated.

### 3.2.1 Definitions of variables and parameters

The fish species population is divided into the following classes (state variables):

- $N_1(t)$ : The biomass of small pelagic fish at any time  $t$
- $N_2(t)$ : The biomass of Nile tilapia at any time  $t$
- $N_3(t)$ : The biomass of Nile perch at any time  $t$

These species  $N_1$ ,  $N_2$ , and  $N_3$  are harvested at rates  $h_1(t)$ ,  $h_2(t)$ , and  $h_3(t)$ , respectively. These rates are called the control variables.

The parameters relating to the interaction between species, growth, and harvesting are defined as follows:

- $r_1$  : The intrinsic growth rate of  $N_1$
- $r_2$  : The intrinsic growth rate of  $N_2$
- $r_3$  : The intrinsic growth rate of  $N_3$
- $K_1$  : The carrying capacity of  $N_1$
- $K_2$  : The carrying capacity of  $N_2$
- $K_3$  : The carrying capacity of  $N_3$
- $n_{32}$ : The growth rate of  $N_3$  due to predation of  $N_2$
- $n_{31}$ : The growth rate of  $N_3$  due to predation of  $N_1$
- $n_{21}$ : The growth rate of  $N_2$  due to predation of  $N_1$
- $n_{23}$ : The consumption rate of  $N_2$  due to its predator  $N_3$
- $n_{13}$ : The consumption rate of  $N_1$  due to its predator  $N_3$
- $n_{12}$ : The consumption rate of  $N_1$  due to its predator  $N_2$

### 3.2.2 Model assumptions

The model relies on the following assumptions.

- (i) Nile perch are predators of both Nile tilapia and small pelagic fish.
- (ii) Small pelagic fish is a prey of Nile tilapia.
- (iii) The predation of Nile perch by Nile tilapia is negligible.

### 3.2.3 Compartmental diagram

The interaction between the three fish species is depicted in Figure 3.1.

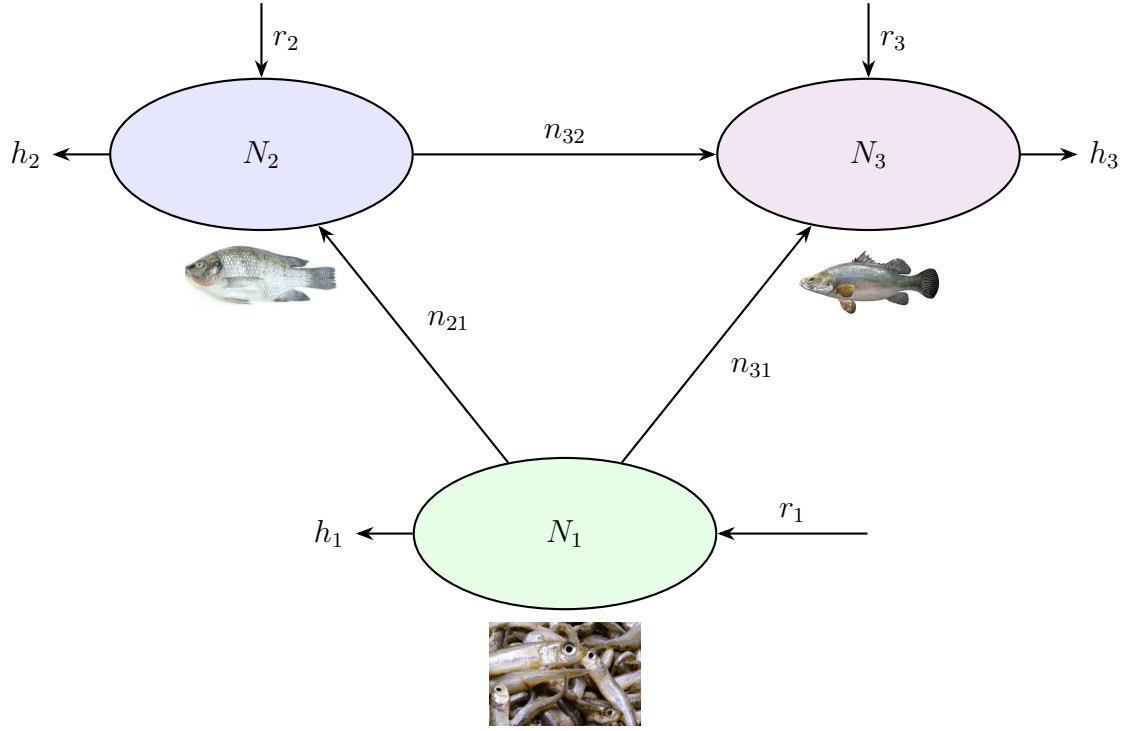


Figure 3.1: The compartmental diagram for the food chain model.

### 3.2.4 The state equations

Using Figure 3.1 and model assumptions, the system of ODEs is obtained as:

$$\begin{cases} \frac{dN_1}{dt} = r_1 N_1 \left(1 - \frac{N_1}{K_1}\right) - n_{13} N_1 N_3 - n_{12} N_1 N_2 - h_1, & N_1(0) = (N_1)_0, \\ \frac{dN_2}{dt} = r_2 N_2 \left(1 - \frac{N_2}{K_2}\right) + n_{21} N_2 N_1 - n_{23} N_2 N_3 - h_2, & N_2(0) = (N_2)_0, \\ \frac{dN_3}{dt} = r_3 N_3 \left(1 - \frac{N_3}{K_3}\right) + n_{32} N_3 N_2 + n_{31} N_3 N_1 - h_3, & N_3(0) = (N_3)_0. \end{cases} \quad (3.1)$$

The terms  $n_{21}N_2N_1$ ,  $n_{31}N_3N_1$ ,  $n_{32}N_3N_2$ ,  $n_{12}N_1N_2$ ,  $n_{13}N_1N_3$ , and  $n_{23}N_2N_3$  represent interaction due to predation between species. The logistic growth of each population is given by

$$r_i N_i \left(1 - \frac{N_i}{K_i}\right), \quad i = 1, 2, 3,$$

which reflects intra-specific competition. Throughout this work, the right-hand side of the ODEs (3.1) is represented by a vector function  $g(t, N)$ .

The state variables  $N_i(t)$ ,  $i = 1, 2, 3$  belong to the space of continuously differentiable

functions over the time interval  $[0, T]$ . This ensures a smooth and well-defined dynamics of the fish population:

$$N_i(t) \in C^1([0, T]) \mid 0 < N_i(t) \leq B_i, \quad i = 1, 2, 3.$$

The symbol  $B_i$  denotes the positive constants representing the upper limits (maximum feasible population sizes) for the different species of fish. The problem (3.1) admits unique solutions (see Theorem 3), but a criterion is required to identify the optimal ones, i.e., those that maximise the net profit of fishing. To this end, the cost functional  $J(h_1, h_2, h_3)$  is introduced.

**Definition 1.** *The cost functional  $J$  is defined as the total revenue minus the cost of fishing:*

$$J(h_1, h_2, h_3) = \int_0^T \sum_{i=1}^3 (p_i h_i - c_i h_i - \mu_i h_i^2) dt, \quad (3.2)$$

where  $J(h_1, h_2, h_3)$  is the net profit of fishing. The term  $p_i h_i$  represents the revenue with unit price  $p_i$ , while  $(c_i h_i + \mu_i h_i^2)$  represents the cost of fishing with  $c_i > 0$  and  $\mu_i > 0$  the coefficients of the linear and quadratic cost terms, respectively, where  $i = 1, 2, 3$ .

The purpose of Definition 1 is to specify the optimal controls  $(h_1^*, h_2^*, h_3^*)$  in  $\mathcal{A}$  that maximise the cost functional (3.2) such that

$$J(h_1^*, h_2^*, h_3^*) = \max_{(h_1, h_2, h_3) \in \mathcal{A}} J(h_1, h_2, h_3).$$

Here,  $\mathcal{A}$  denotes the class of admissible controls given by

$$\mathcal{A} = \left\{ h(t) = (h_1(t), h_2(t), h_3(t)) : [0, T] \rightarrow \mathbb{R}^3 \left| \begin{array}{l} h_i \text{ is Lebesgue measurable, } 0 \leq h_i(t) \leq M_i, \\ M_i \in \mathbb{R}^{\geq 0}, \text{ and } i = 1, 2, 3 \end{array} \right. \right\}. \quad (3.3)$$

### 3.3 Existence and Uniqueness of State Solutions

In this section, the existence and uniqueness of the solution for the state system (3.1) were proven. These ensure that the state solutions are well-posed and suitable for numerical simulations.

**Theorem 1** (Peano's Existence Theorem). *If the function  $g(t, N)$  is continuous in a neighborhood of  $t = 0$ , where  $N = (N_1, N_2, N_3)^T$ , then the initial value problem (3.1) has at least one solution defined in a neighborhood of  $t = 0$ .*

A comprehensive and accessible modern proof of Theorem 1, along with several important refinements, can be found in Pouso (2012).

**Lemma 2.** *Let  $E$  be a convex domain and  $g : E \rightarrow \mathbb{R}$ . Suppose the partial derivatives  $\frac{\partial g}{\partial N_i}$ ,  $i = 1, 2, 3$ , exist and*

$$\sup_{(t,N) \in E} \left\| \frac{\partial g}{\partial N} \right\|_1 \leq L,$$

where  $N = (N_1, N_2, N_3)^T$ . Then the function  $g(t, N)$  satisfies the Lipschitz condition

$$\|g(t, N) - g(t, M)\|_2 \leq L \|N - M\|_2, \quad \forall (t, N), (t, M) \in E.$$

*Proof.* The system of ODEs (3.1) can be rewritten as:

$$\frac{dN}{dt} = g(t, N),$$

where  $g(t, N)$  is given by

$$g(t, N) = \begin{pmatrix} r_1 N_1 \left(1 - \frac{N_1}{K_1}\right) - n_{13} N_1 N_3 - n_{12} N_1 N_2 - h_1 \\ r_2 N_2 \left(1 - \frac{N_2}{K_2}\right) + n_{21} N_2 N_1 - n_{23} N_2 N_3 - h_2 \\ r_3 N_3 \left(1 - \frac{N_3}{K_3}\right) + n_{32} N_3 N_2 + n_{31} N_3 N_1 - h_3 \end{pmatrix}.$$

Since

$$\frac{\partial g}{\partial N_1} = \begin{pmatrix} r_1 \left(1 - \frac{2N_1}{K_1}\right) - n_{13} N_3 - n_{12} N_2 \\ n_{21} N_2 \\ n_{31} N_3 \end{pmatrix} = \begin{pmatrix} a_{11} \\ a_{21} \\ a_{31} \end{pmatrix},$$

$$\frac{\partial g}{\partial N_2} = \begin{pmatrix} -n_{12} N_1 \\ r_2 \left(1 - \frac{2N_2}{K_2}\right) + n_{21} N_1 - n_{23} N_3 \\ n_{32} N_3 \end{pmatrix} = \begin{pmatrix} a_{12} \\ a_{22} \\ a_{32} \end{pmatrix},$$

and

$$\frac{\partial g}{\partial N_3} = \begin{pmatrix} -n_{13} N_1 \\ -n_{23} N_2 \\ r_3 \left(1 - \frac{2N_3}{K_3}\right) + n_{32} N_2 + n_{31} N_1 \end{pmatrix} = \begin{pmatrix} a_{13} \\ a_{23} \\ a_{33} \end{pmatrix},$$

then

$$\left\| \frac{\partial g}{\partial N} \right\|_1 = \max \{ (|a_{11}| + |a_{21}| + |a_{31}|), (|a_{12}| + |a_{22}| + |a_{32}|), (|a_{13}| + |a_{23}| + |a_{33}|) \} = L,$$

where  $L$  is a nonnegative Lipschitz constant and  $\|\cdot\|_1$  denotes the 1-norm (Refer to Appendix A for the definition).

This implies that  $\sup_{(t,N) \in E} \left\| \frac{\partial g}{\partial N} \right\|_1 \leq L$ . Since  $\frac{\partial g}{\partial N_i}$ ,  $i = 1, 2, 3$  exist and  $\sup_{(t,N) \in E} \left\| \frac{\partial g}{\partial N} \right\|_1 \leq L$ ,  $g(t, N)$  satisfies the Lipschitz condition (Agarwal & O'Regan, 2008, pg. 46-47).  $\square$

**Theorem 3** (Lipschitz Uniqueness Theorem). *Let the function  $g(t, N)$  be continuous for all  $(t, N) \in E$ . If  $g(t, N)$  satisfies the Lipschitz condition in Lemma 2, then the initial value problem (3.1) admits a unique solution in a neighborhood of  $t = 0$ .*

From Lemma 2,  $g(t, N)$  satisfies the Lipschitz condition, which implies that the initial value problem (3.1) has a unique solution in a neighborhood of  $t_0$  (Agarwal & O'Regan, 2008, pg. 68). According to Theorem 1 and Theorem 3, there exist unique state solutions. In the next section, the existence and uniqueness of optimal controls are shown. This ensures that unique optimal controls exist within a class of admissible control (3.3).

### 3.4 Existence and Uniqueness of the Optimal Controls

This section shows that there exists a unique optimal control  $h_i^*(t)$  and associated state solution  $N_i^*(t)$  to the optimal control problem (3.1)-(3.2) for  $i = 1, 2, 3$ .

**Theorem 4.** *Suppose  $(N_i^*(t), h_i^*(t))$ ,  $i = 1, 2, 3$ , is an admissible pair. If the admissible control set  $\mathcal{A}$  is convex and the cost functional  $J(h_1, h_2, h_3)$  is strictly concave in  $(h_1, h_2, h_3)$ , then there exists a unique optimal control  $(h_1^*, h_2^*, h_3^*) \in \mathcal{A}$  such that*

$$J(h_1^*, h_2^*, h_3^*) = \max_{(h_1, h_2, h_3) \in \mathcal{A}} J(h_1, h_2, h_3).$$

*Proof.* The admissible control  $\mathcal{A}$  is convex because it is defined linearly in terms of the control variables  $h_i(t)$ ,  $i = 1, 2, 3$ . The cost functional  $J$ , in Definition 1, is strictly concave in  $h_i(t)$ ,  $i = 1, 2, 3$ , due to the negative quadratic terms  $-\mu_i h_i^2$  with  $-\mu_i < 0$ . Moreover, it is independent of the state variables  $N_i(t)$ ,  $i = 1, 2, 3$ . In view of (Lenhart & Workman, 2007, pg. 26), the strict concavity of  $J$  over the convex set  $\mathcal{A}$  guarantees the existence of a unique optimal control  $(h_1^*, h_2^*, h_3^*)$  that maximises  $J$ .  $\square$

### 3.5 Positivity and Boundedness of the State Solutions

In this section, the positivity and uniform boundedness of the state solutions are demonstrated. These ensure that the fish population stays above zero and grows within biolog-

ically feasible limits, given space and resource constraints.

**Theorem 5.** *Suppose  $N_1(t)$ ,  $N_2(t)$ , and  $N_3(t)$ , are the solutions of the state system (3.1), then there exist constants  $B_1, B_2, B_3 > 0$  such that*

$$0 < N_1(t) \leq B_1, \quad 0 < N_2(t) \leq B_2, \quad 0 < N_3(t) \leq B_3, \quad \forall t \in [0, T].$$

*Proof.* First,  $0 < N_1(t) \leq B_1$  for all  $t \in [0, T]$  is shown. The differential equation involving  $N_1$  in equation (3.1) is given by:

$$\frac{dN_1}{dt} = r_1 N_1 \left( 1 - \frac{N_1}{K_1} \right) - n_{13} N_1 N_3 - n_{12} N_1 N_2 - h_1. \quad (3.4)$$

Note that (3.4) can be modified using the substitution:

$$N_1 = \frac{1}{\hat{N}_1}, \quad (3.5)$$

Differentiating (3.5) with respect to  $t$  yields:

$$\frac{dN_1}{dt} = -\frac{1}{\hat{N}_1^2} \frac{d\hat{N}_1}{dt}. \quad (3.6)$$

Substituting (3.5) and (3.6) into equation (3.4), gives

$$-\frac{1}{\hat{N}_1^2} \frac{d\hat{N}_1}{dt} = r_1 \frac{1}{\hat{N}_1} \left( 1 - \frac{1}{K_1 \hat{N}_1} \right) - n_{13} N_3 \frac{1}{\hat{N}_1} - n_{12} N_2 \frac{1}{\hat{N}_1} - h_1. \quad (3.7)$$

Equation (3.7) is multiplied through by  $-\hat{N}_1^2$  to obtain

$$\frac{d\hat{N}_1}{dt} = -r_1 \hat{N}_1 + \frac{r_1}{K_1} + n_{13} N_3 \hat{N}_1 + n_{12} N_2 \hat{N}_1 + h_1 \hat{N}_1^2. \quad (3.8)$$

Simplifying (3.8), yields

$$\frac{d\hat{N}_1}{dt} = (-r_1 + n_{13} N_3 + n_{12} N_2) \hat{N}_1 + \frac{r_1}{K_1} + h_1 \hat{N}_1^2. \quad (3.9)$$

Let  $(-r_1 + n_{13} N_3 + n_{12} N_2) = \phi(N_2, N_3)$  in equation (3.9). Then neglecting the positive terms  $\frac{r_1}{K_1}$  and  $h_1 \hat{N}_1^2$  in (3.9) implies

$$\frac{d\hat{N}_1}{dt} \geq \phi(N_2, N_3) \hat{N}_1. \quad (3.10)$$

On integrating (3.10) over  $t \in [0, T]$  using separation of variables, gives

$$\hat{N}_1(t) \geq (\hat{N}_1)_0 e^{\int_0^t \phi(N_2, N_3) dt}. \quad (3.11)$$

Since  $(\hat{N}_1)_0 > 0$  and  $e^{\int_0^t \phi(N_2, N_3) dt} > 0$  in (3.11), it follows that  $\hat{N}_1(t) > 0$  for each  $t \in [0, T]$ . Using  $\hat{N}_1(t) > 0$  in (3.5) implies

$$N_1(t) > 0 \quad \text{for each } t \in [0, T]. \quad (3.12)$$

Next, an upper bound of  $N_1(t)$  over the time interval  $[0, T]$  is shown. Since all the coefficients are positive and the state variable  $N_1(t) > 0$  for every  $t \in [0, T]$ , equation (3.4) can be written as:

$$\frac{dN_1}{dt} = r_1 N_1 \left(1 - \frac{N_1}{K_1}\right) - n_{13} N_1 N_3 - n_{12} N_1 N_2 - h_1 \leq r_1 N_1 \left(1 - \frac{N_1}{K_1}\right) \leq r_1 N_1.$$

Thus,

$$\frac{dN_1}{dt} \leq r_1 N_1. \quad (3.13)$$

Integrating (3.13) using separation of variables over  $[0, T]$ , yields

$$N_1(t) \leq (N_1)_0 e^{r_1 t}, \quad \forall t \in [0, T]. \quad (3.14)$$

Note that  $e^{r_1 t} \leq e^{r_1 T}$  for every  $t \in [0, T]$ . Thus,

$$N_1(t) \leq (N_1)_0 e^{r_1 t} \leq (N_1)_0 e^{r_1 T} := B_1, \quad \text{for every } t \in [0, T]. \quad (3.15)$$

Combining (3.12) and (3.15), gives

$$0 < N_1(t) \leq B_1, \quad \forall t \in [0, T].$$

Using similar arguments, it follows that

$$0 < N_2(t) \leq B_2, \quad 0 < N_3(t) \leq B_3, \quad \forall t \in [0, T]. \quad (3.16)$$

Hence, the state solution  $N_i(t)$  is positive and uniformly bounded for every  $t \in [0, T]$  and each  $i = 1, 2, 3$ .  $\square$

## 3.6 The Optimality System

The optimality system is derived using Pontryagin's maximum principle (Pontryagin et al., 1967). It comprises the state system, the adjoint system, and the optimality condition. The Hamiltonian  $\mathcal{H}$  is formulated by incorporating the state equations (3.1) and the cost functional (3.2).

**Definition 2.** *The Hamiltonian  $\mathcal{H}$  is defined as*

$$\begin{aligned} \mathcal{H} = & (p_1 h_1 - c_1 h_1 - \mu_1 h_1^2) + (p_2 h_2 - c_2 h_2 - \mu_2 h_2^2) + (p_3 h_3 - c_3 h_3 - \mu_3 h_3^2) \\ & + \lambda_1 \left( r_1 N_1 \left( 1 - \frac{N_1}{K_1} \right) - n_{13} N_1 N_3 - n_{12} N_1 N_2 - h_1 \right) \\ & + \lambda_2 \left( r_2 N_2 \left( 1 - \frac{N_2}{K_2} \right) + n_{21} N_2 N_1 - n_{23} N_2 N_3 - h_2 \right) \\ & + \lambda_3 \left( r_3 N_3 \left( 1 - \frac{N_3}{K_3} \right) + n_{32} N_3 N_2 + n_{31} N_3 N_1 - h_3 \right). \end{aligned} \quad (3.17)$$

The symbols  $\lambda_1(t)$ ,  $\lambda_2(t)$ , and  $\lambda_3(t)$  represent the adjoint variables associated with their states  $N_1(t)$ ,  $N_2(t)$ , and  $N_3(t)$ , respectively.

### 3.6.1 Adjoint equations

Following the technique in Lenhart & Workman (2007), the adjoint equations are determined using the Hamiltonian (3.17) as

$$\frac{d\lambda_1}{dt} = -\frac{\partial \mathcal{H}}{\partial N_1}, \quad \frac{d\lambda_2}{dt} = -\frac{\partial \mathcal{H}}{\partial N_2}, \quad \frac{d\lambda_3}{dt} = -\frac{\partial \mathcal{H}}{\partial N_3}.$$

This results into:

$$\begin{cases} \frac{d\lambda_1}{dt} = - \left[ \lambda_1 \left( r_1 \left( 1 - \frac{2N_1}{K_1} \right) - n_{13} N_3 - n_{12} N_2 \right) + \lambda_2 n_{21} N_2 + \lambda_3 n_{31} N_3 \right], \\ \frac{d\lambda_2}{dt} = - \left[ -\lambda_1 n_{12} N_1 + \lambda_2 \left( r_2 \left( 1 - \frac{2N_2}{K_2} \right) + n_{21} N_1 - n_{23} N_3 \right) + \lambda_3 n_{32} N_3 \right], \\ \frac{d\lambda_3}{dt} = - \left[ -\lambda_1 n_{13} N_1 - \lambda_2 n_{23} N_2 + \lambda_3 \left( r_3 \left( 1 - \frac{2N_3}{K_3} \right) + n_{32} N_2 + n_{31} N_1 \right) \right], \\ \lambda_i(T) = 0, \quad i = 1, 2, 3. \end{cases} \quad (3.18)$$

### 3.6.2 Optimality condition

To obtain the optimality condition, the Hamiltonian (3.17) is first partially differentiated with respect to the control variables  $h_1$ ,  $h_2$ , and  $h_3$ :

$$\begin{cases} \frac{\partial \mathcal{H}}{\partial h_1} = p_1 - c_1 - 2\mu_1 h_1 - \lambda_1, \\ \frac{\partial \mathcal{H}}{\partial h_2} = p_2 - c_2 - 2\mu_2 h_2 - \lambda_2, \\ \frac{\partial \mathcal{H}}{\partial h_3} = p_3 - c_3 - 2\mu_3 h_3 - \lambda_3. \end{cases} \quad (3.19)$$

Differentiating the 1st, 2nd, and 3rd equations in (3.19) with respect to  $h_1$ ,  $h_2$ , and  $h_3$ , respectively, yields:

$$\begin{aligned} \frac{\partial^2 \mathcal{H}}{\partial h_1^2} &= -2\mu_1, \\ \frac{\partial^2 \mathcal{H}}{\partial h_2^2} &= -2\mu_2, \\ \frac{\partial^2 \mathcal{H}}{\partial h_3^2} &= -2\mu_3. \end{aligned}$$

Since  $\mu_1$ ,  $\mu_2$ , and  $\mu_3$  are positive, then

$$\frac{\partial^2 \mathcal{H}}{\partial h_1^2} < 0, \quad \frac{\partial^2 \mathcal{H}}{\partial h_2^2} < 0, \quad \frac{\partial^2 \mathcal{H}}{\partial h_3^2} < 0.$$

Hence, a maximisation problem. To maximise the Hamiltonian with respect to the controls  $h_i(t)$ ,  $i = 1, 2, 3$ , there are three distinct cases to characterise the optimal controls  $h_i^*$ ,  $i = 1, 2, 3$  as follows (Lenhart & Workman, 2007).

$$h_i^*(t) = \begin{cases} 0 & ; \quad \frac{\partial \mathcal{H}}{\partial h_i} < 0, \\ 0 \leq h_i^*(t) \leq M_i & ; \quad \frac{\partial \mathcal{H}}{\partial h_i} = 0, \\ M_i & ; \quad \frac{\partial \mathcal{H}}{\partial h_i} > 0, \end{cases} \quad (3.20)$$

where  $i = 1, 2, 3$ . Next, each of the three cases is considered as follows.

Case 1. Using  $\frac{\partial \mathcal{H}}{\partial h_1} = 0$ ,  $\frac{\partial \mathcal{H}}{\partial h_2} = 0$ , and  $\frac{\partial \mathcal{H}}{\partial h_3} = 0$  in (3.19), gives

$$\begin{cases} \frac{\partial \mathcal{H}}{\partial h_1} = p_1 - c_1 - 2\mu_1 h_1 - \lambda_1 = 0, \\ \frac{\partial \mathcal{H}}{\partial h_2} = p_2 - c_2 - 2\mu_2 h_2 - \lambda_2 = 0, \\ \frac{\partial \mathcal{H}}{\partial h_3} = p_3 - c_3 - 2\mu_3 h_3 - \lambda_3 = 0. \end{cases} \quad (3.21)$$

Solving (3.21) for  $h_1$ ,  $h_2$ , and  $h_3$  yields the optimal harvest rates  $h_1^*$ ,  $h_2^*$ , and  $h_3^*$ , respectively:

$$\begin{aligned} h_1^* &= \frac{p_1 - c_1 - \lambda_1}{2\mu_1}, \\ h_2^* &= \frac{p_2 - c_2 - \lambda_2}{2\mu_2}, \\ h_3^* &= \frac{p_3 - c_3 - \lambda_3}{2\mu_3}. \end{aligned}$$

This implies

$$\begin{cases} 0 \leq h_1^*(t) = \frac{p_1 - c_1 - \lambda_1}{2\mu_1} \leq M_1 & t \in [0, T], \\ 0 \leq h_2^*(t) = \frac{p_2 - c_2 - \lambda_2}{2\mu_2} \leq M_2 & t \in [0, T], \\ 0 \leq h_3^*(t) = \frac{p_3 - c_3 - \lambda_3}{2\mu_3} \leq M_3 & t \in [0, T]. \end{cases} \quad (3.22)$$

Case 2. Using  $\frac{\partial \mathcal{H}}{\partial h_1} < 0$ ,  $\frac{\partial \mathcal{H}}{\partial h_2} < 0$ , and  $\frac{\partial \mathcal{H}}{\partial h_3} < 0$  with  $h_1^* = h_2^* = h_3^* = 0$  in (3.19), gives

$$\begin{cases} \frac{\partial \mathcal{H}}{\partial h_1} = p_1 - c_1 - \lambda_1 < 0, \\ \frac{\partial \mathcal{H}}{\partial h_2} = p_2 - c_2 - \lambda_2 < 0, \\ \frac{\partial \mathcal{H}}{\partial h_3} = p_3 - c_3 - \lambda_3 < 0. \end{cases} \quad (3.23)$$

Since  $\mu_i > 0$  for each  $i = 1, 2, 3$ , (3.23) reduces to

$$\begin{aligned} \frac{p_1 - c_1 - \lambda_1}{2\mu_1} < 0 &= h_1(t), & t \in [0, T], \\ \frac{p_2 - c_2 - \lambda_2}{2\mu_2} < 0 &= h_2(t), & t \in [0, T], \\ \frac{p_3 - c_3 - \lambda_3}{2\mu_3} < 0 &= h_3(t), & t \in [0, T]. \end{aligned}$$

Therefore:

$$\begin{cases} h_1^*(t) = \max\left(0, \frac{p_1 - c_1 - \lambda_1}{2\mu_1}\right), & t \in [0, T], \\ h_2^*(t) = \max\left(0, \frac{p_2 - c_2 - \lambda_2}{2\mu_2}\right), & t \in [0, T], \\ h_3^*(t) = \max\left(0, \frac{p_3 - c_3 - \lambda_3}{2\mu_3}\right), & t \in [0, T]. \end{cases} \quad (3.24)$$

Case 3. Using  $\frac{\partial \mathcal{H}}{\partial h_1} > 0$ ,  $\frac{\partial \mathcal{H}}{\partial h_2} > 0$ , and  $\frac{\partial \mathcal{H}}{\partial h_3} > 0$  with  $h_1^* = M_1$ ,  $h_2^* = M_2$ , and  $h_3^* = M_3$  in (3.19), yields

$$\begin{cases} p_1 - c_1 - 2\mu_1 M_1 - \lambda_1 > 0, \\ p_2 - c_2 - 2\mu_2 M_2 - \lambda_2 > 0, \\ p_3 - c_3 - 2\mu_3 M_3 - \lambda_3 > 0. \end{cases} \quad (3.25)$$

Since  $\mu_1$ ,  $\mu_2$ , and  $\mu_3$  are positive, (3.25) is rearranged as:

$$\begin{aligned} \frac{p_1 - c_1 - \lambda_1}{2\mu_1} &> M_1 = h_1(t), \quad t \in [0, T], \\ \frac{p_2 - c_2 - \lambda_2}{2\mu_2} &> M_2 = h_2(t), \quad t \in [0, T], \\ \frac{p_3 - c_3 - \lambda_3}{2\mu_3} &> M_3 = h_3(t), \quad t \in [0, T]. \end{aligned}$$

Thus:

$$\begin{cases} h_1^*(t) = \min \left( M_1, \frac{p_1 - c_1 - \lambda_1}{2\mu_1} \right), \quad t \in [0, T], \\ h_2^*(t) = \min \left( M_2, \frac{p_2 - c_2 - \lambda_2}{2\mu_2} \right), \quad t \in [0, T], \\ h_3^*(t) = \min \left( M_3, \frac{p_3 - c_3 - \lambda_3}{2\mu_3} \right), \quad t \in [0, T]. \end{cases} \quad (3.26)$$

Considering these three cases (3.22), (3.24), and (3.26), the optimality condition is obtained as

$$\begin{cases} h_1^*(t) = \min \left( M_1, \max \left( 0, \frac{p_1 - c_1 - \lambda_1^*}{2\mu_1} \right) \right), \quad t \in [0, T], \\ h_2^*(t) = \min \left( M_2, \max \left( 0, \frac{p_2 - c_2 - \lambda_2^*}{2\mu_2} \right) \right), \quad t \in [0, T], \\ h_3^*(t) = \min \left( M_3, \max \left( 0, \frac{p_3 - c_3 - \lambda_3^*}{2\mu_3} \right) \right), \quad t \in [0, T]. \end{cases} \quad (3.27)$$

The optimality system consists of the state system (3.1), the adjoint equations (3.18), and the optimality condition (3.27).

### 3.7 Parameter Estimation

The parameters used in the model are estimated in this section. The price parameters for the three fish species were estimated on the basis of recent retail market data. According to the Uganda Bureau of Statistics [UBOS \(2024\)](#), the average price of small pelagic fish is US\$ 22,724 per kilogram. For Nile tilapia, estimated within the range of US\$ 11,603.42–24,189.54 per kilogram ([Selina Wamuci, 2025b](#)). Similarly, for Nile perch, it was estimated within the reported price range of US\$ 155,190–369,500 per kilogram ([Selina Wamuci, 2025a](#)). The values in [Table 3.1](#) are the price of fish per tonne.

According to [Namukonge and Barakagira \(2024\)](#), the total operating cost during fish production was US\$ 34,528,400, with an average harvest of 8,000 fish weighing 0.7 kg each, totaling 5,600 kg. This results in an average cost of approximately US\$ 6,166 per kilogram in the year 2024. In this study, the cost of harvesting Nile perch is significantly estimated to be higher than that of Nile tilapia, reflecting its high commercial value and associated processing expenses. In contrast, small pelagic fish had a much lower estimate, mainly due to their high catchability rate compared to that of Nile perch and Nile tilapia within the same lake ([Mpele et al., 2014a](#)). The values in [Table 3.1](#) represent the total cost of harvesting and processing, which were scaled to cost per unit tonne.

The quadratic cost coefficients were deliberately chosen to be much lower than the linear cost coefficient. This reflects the reality that most harvesting costs, such as fuel, labor, and gear maintenance, are largely proportional to the level of fishing effort and thus scale approximately linearly with the harvest. However, including a small quadratic cost term models the increasing marginal costs that arise when fish become less abundant, causing the cost per additional unit harvested to rise.

To estimate the carrying capacity of the fish species for Lake Albert (Uganda's portion), values from Lake Victoria were scaled based on surface area. Lake Victoria covers 68,800 km<sup>2</sup>, while Uganda encompasses 2,438 km<sup>2</sup> of Lake Albert ([Brilliant, 2025](#)), approximately 3.544% of Lake Victoria. Using the scaling factor of 0.03544, the carrying capacities of Lake Victoria fish species were scaled to estimate those of Lake Albert, Uganda. In addition, the carrying capacity per square kilometer was found by dividing the previous values by Lake Albert's total surface area of 2,438 km<sup>2</sup>. Based on this adjustment, the estimated carrying capacities for Lake Albert are derived from the original values reported for Lake Victoria by [Mpele et al. \(2014b\)](#). [Table 3.1](#) summarises all the parameters and their sources.

Table 3.1: Parameter descriptions and values under constant yield harvesting strategies.

Parameter	Description	Value	Source
$r_1$	Intrinsic growth rate of $N_1$	0.6546	Mpele et al. (2014b)
$r_2$	Intrinsic growth rate of $N_2$	0.1112	Mpele et al. (2014b)
$r_3$	Intrinsic growth rate of $N_3$	0.4770	Mpele et al. (2014b)
$n_{32}$	Growth rate of $N_3$ due to predation of $N_2$	0.004	Estimated
$n_{23}$	Consumption rate of $N_2$ due to its predator $N_3$	0.004	Estimated
$n_{31}$	Growth rate of $N_3$ due to predation of $N_1$	0.005	Mpele et al. (2014a)
$n_{13}$	Consumption rate of $N_1$ due to its predator $N_3$	0.005	Mpele et al. (2014a)
$n_{21}$	Growth rate of $N_2$ due to predation of $N_1$	0.005	Mpele et al. (2014a)
$n_{12}$	Consumption rate of $N_1$ due to its predator $N_2$	0.005	Mpele et al. (2014a)
$K_1$	Carrying capacity of $N_1$	38.24 tons	Estimated
$K_2$	Carrying capacity of $N_2$	3.54 tons	Estimated
$K_3$	Carrying capacity of $N_3$	9.36 tons	Estimated
$p_1$	Price per unit biomass of $N_1$	USh $22.7 \times 10^6$	Estimated
$p_2$	Price per unit biomass of $N_2$	USh $24.0 \times 10^6$	Estimated
$p_3$	Price per unit biomass of $N_3$	USh $200 \times 10^6$	Estimated
$c_1$	Linear cost coefficient for $N_1$	USh $10.0 \times 10^6$	Estimated
$c_2$	Linear cost coefficient for $N_2$	USh $19.0 \times 10^6$	Estimated
$c_3$	Linear cost coefficient for $N_3$	USh $150 \times 10^6$	Estimated
$\mu_1$	Quadratic cost coefficient for $N_1$	USh $4.0 \times 10^6$	Estimated
$\mu_2$	Quadratic cost coefficient for $N_2$	USh $7.0 \times 10^6$	Estimated
$\mu_3$	Quadratic cost coefficient for $N_3$	USh $14 \times 10^6$	Estimated

### 3.8 Numerical Simulations

The model was formulated using nonlinear ODEs (3.1), subject to constant yield harvesting and incorporating logistic growth and prey-predator interactions, among the three fish species. The cost functional (3.2) in Definition 1 is used to maximise the net value of fishing for the three species by balancing the benefits of harvesting with the associated costs. Furthermore, the existence and uniqueness of the state solutions were proven, using Theorem 1 and Theorem 3, respectively. The existence and uniqueness of the optimal control are proven using Theorem 4. The positivity and boundedness of the state solutions were proven. Additionally, the optimality system is derived using the PMP and subsequently solved using the forward-backward sweep method, implemented with the fourth-order Runge-Kutta scheme; detailed MATLAB code is provided in Appendix B.

### 3.8.1 Optimal solutions

Performing numerical simulations using the forward-backward sweep with parameter values in Table 3.1, the optimal solutions are presented in Figure 3.2 and Table 3.2. From Figure 3.2(a), it is observed that the harvest rates for the fish species remain constant over the simulation period, indicating that the harvest rates are independent of the fish biomass. The highest harvest rate is recorded for Nile perch, followed by small pelagic fish, and the lowest harvest rate is for Nile tilapia. The highest harvest rate for Nile perch leads to a reduction in the predation pressure on species at lower trophic levels, thus contributing to the balance of the ecosystem. The lowest rate ensures that the prey population does not go to extinction.

The dynamics of fish population presented in Figure 3.2(b) reveal that the biomass of small pelagic fish increases rapidly due to high intrinsic growth rate and low initial biomass compared to its carrying capacity. However, the optimal biomass is attained below the carrying capacity as a result of predation and harvest. Considering the population of Nile tilapia, its biomass decreases due to its low intrinsic growth rate and vulnerability to both harvest and predation by Nile perch. The optimal biomass is attained above its carrying capacity due to the low optimal harvest rate. For Nile perch, the biomass decreases as a result of harvest and intra-species competition. The slight increase before the optimal level is due to its predatory role in feeding on the two fish species. The optimal biomass remains lower than the carrying capacity because of its high harvest rate.

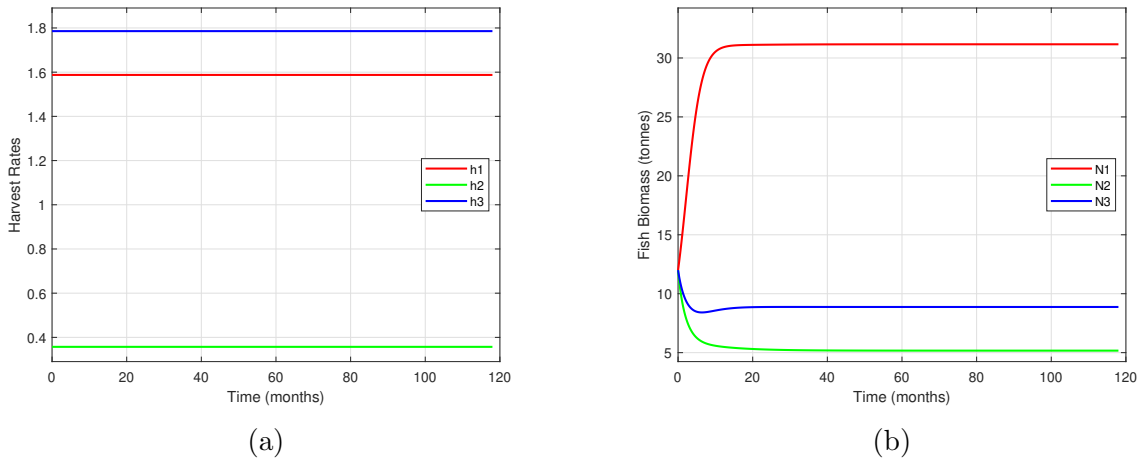


Figure 3.2: (a) Optimal harvest rate and (b) Biomass of small pelagic fish, Nile tilapia, and Nile perch under constant yield harvesting strategies.

The summary of optimal solutions for the three fish species, as illustrated in Figure 3.2, is shown in Table 3.2.

Table 3.2: Summary of the results for the optimal solutions under constant yield harvesting strategies.

Optimal solution	Fish species	Optimal value (tonnes)
Harvest Rate	Small pelagic fish, $h_1^*$	1.58750
	Nile tilapia, $h_2^*$	0.35714
	Nile perch, $h_3^*$	1.78571
Fish Biomass	Small pelagic fish, $N_1^*$	31.16119
	Nile tilapia, $N_2^*$	5.17132
	Nile perch, $N_3^*$	8.87502

### 3.8.2 Dynamics of fish populations with different harvest rates

The effects of varying harvest rates on the dynamics of each fish population for three different harvest levels are presented, as illustrated in Figure 3.3. Specifically, the dynamics of fish populations are compared for optimal harvest rates  $h_i^*$ ,  $i = 1, 2, 3$  obtained from Table 3.2, with that of increased harvest rates  $1.5h_i^*$  (above optimal), and reduced harvest rates  $0.5h_i^*$  (below optimal). Figure 3.3 shows that fish biomass increases as harvest rates decrease and vice versa. At optimal harvest rates, all species of fish achieve a sustainable balance between ecological stability and economic benefit. Harvesting below optimal levels results in a further increase in fish biomass for the three species of fish, indicating improved biological conservation but potentially reduced economic returns. In contrast, exceeding optimal harvest rates causes a significant reduction in fish biomass, reflecting overexploitation and potential long-term ecological harm. The extinction of the super predator  $N_3$  seen in Figure 3.3(c), causes abnormal increase in the biomass of  $N_1$  and  $N_2$  in Figure 3.3(a) and Figure 3.3(b), respectively, at the point of extinction.

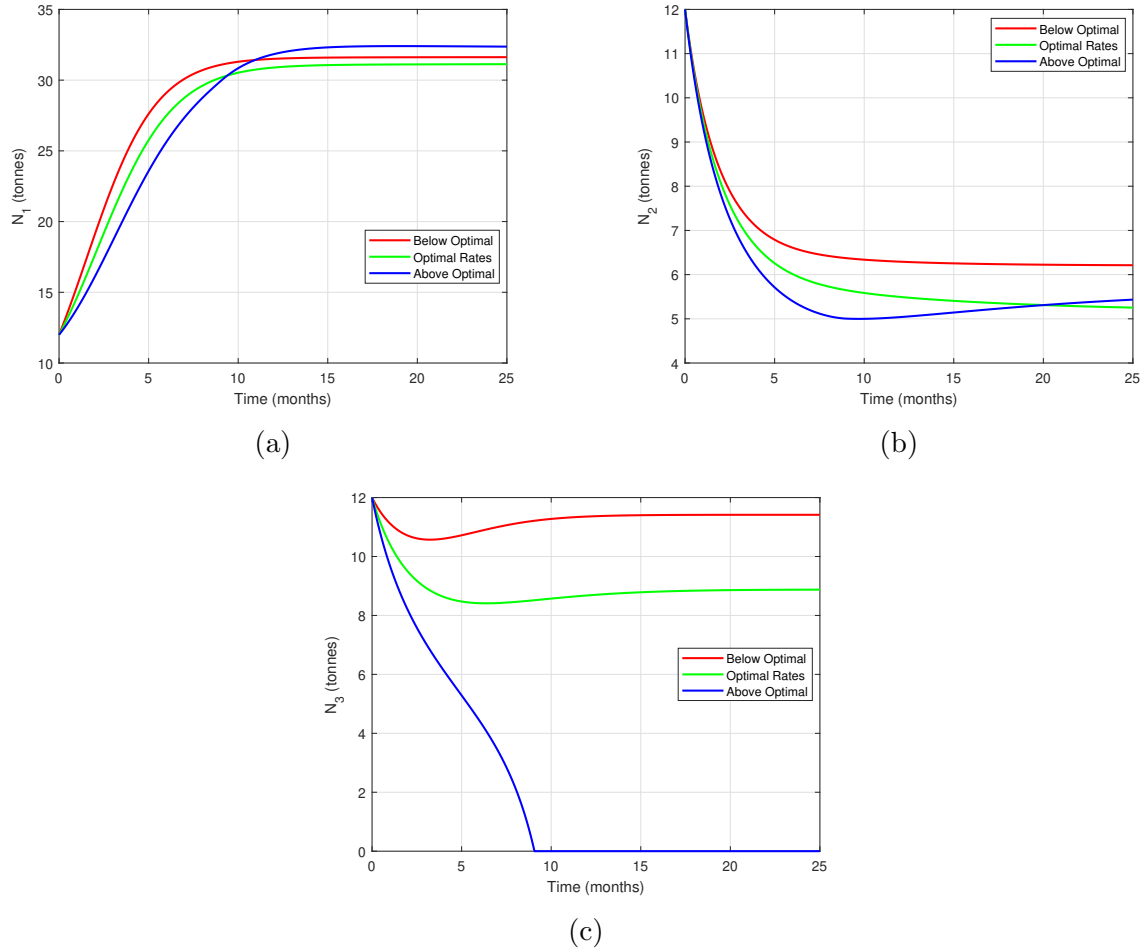
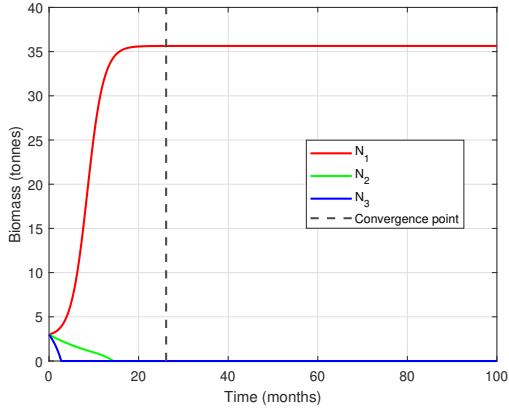


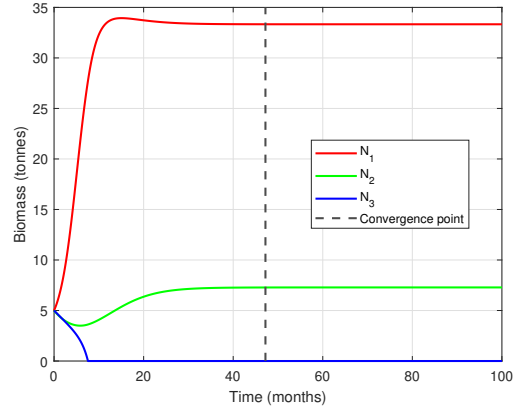
Figure 3.3: Variation of fish populations with time for different harvest rates: (a) small pelagic fish, (b) Nile tilapia, (c) Nile perch

### 3.8.3 The influence of different initial biomass on the dynamics of fish populations

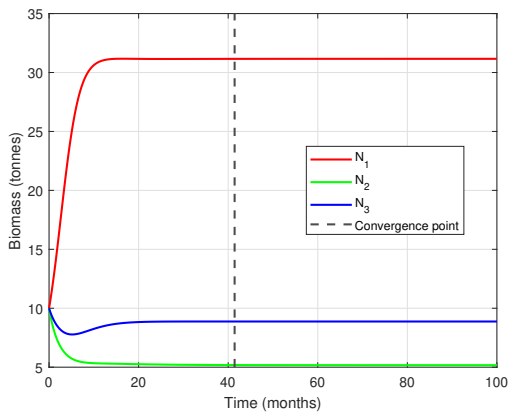
The effects of varying initial biomass on the dynamics of each fish population at optimal harvest rates are presented in Figure 3.4. Figure 3.4((a) and (b)) shows that at low initial biomass, fish species are at risk of extinction, especially predators, as a result of high competition for the few available resources. In Figure 3.4(c), the moderate initial biomass converges faster compared to the high initial biomass, which takes a relatively longer simulation time to converge, as shown in Figure 3.4(d). When predators go extinct, as shown in Figure 3.4 ((a), (b), and (e)), the remaining species stabilise above the optimal levels as a result of reduced predator pressure. Figure 3.4(f) shows that at very low initial biomass of the prey, all species go to extinction as a result of intra-species competition for limited prey.



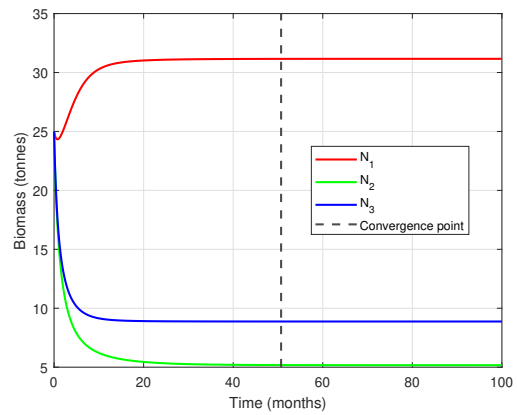
(a)  $(N_1)_0 = 3$ ,  $(N_2)_0 = 3$ , and  $(N_3)_0 = 3$



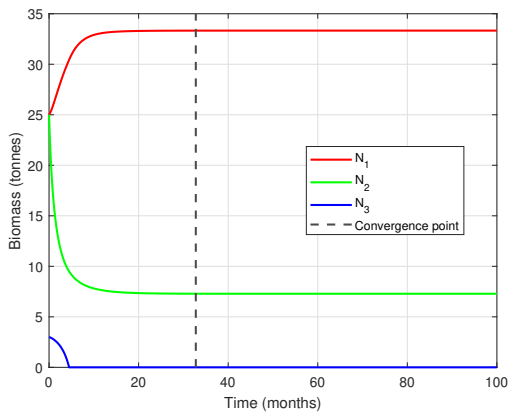
(b)  $(N_1)_0 = 5$ ,  $(N_2)_0 = 5$ , and  $(N_3)_0 = 5$



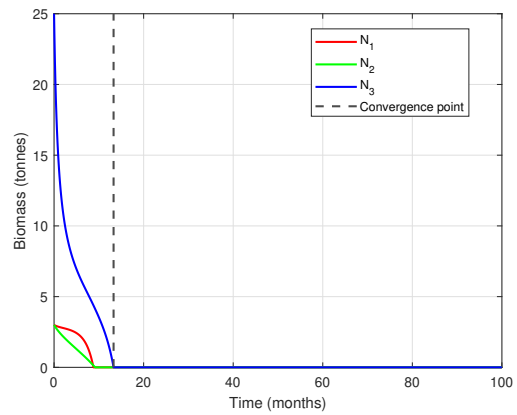
(c)  $(N_1)_0 = 10$ ,  $(N_2)_0 = 10$ , and  $(N_3)_0 = 10$



(d)  $(N_1)_0 = 25$ ,  $(N_2)_0 = 25$ , and  $(N_3)_0 = 25$



(e)  $(N_1)_0 = 25$ ,  $(N_2)_0 = 25$ , and  $(N_3)_0 = 3$



(f)  $(N_1)_0 = 3$ ,  $(N_2)_0 = 3$ , and  $(N_3)_0 = 25$

Figure 3.4: Variation of fish populations with time for different initial conditions ( $2 \leq (N_i)_0 \leq 30$   $i = 1, 2, 3$ )

# Chapter 4

## The Optimal Conditions for the Co-existence of Fish Populations under Constant Effort Harvesting Model

### 4.1 Introduction

In this chapter, the optimal harvesting strategies of fish populations modelled with constant effort harvesting are presented. The layout of this chapter is as follows. Formulation of the model, followed by a theoretical investigation of the existence and uniqueness of the state and control variables. Next, the positivity and boundedness of the state solutions are analysed. In addition, the optimality system is derived. Finally, approximation using the fourth-order Runge-Kutta method, parameter estimations, and numerical simulations are presented.

### 4.2 Model Formulation

In this section, the optimal harvesting strategies for fish populations governed by three sets of nonlinear ODEs subjected to constant effort harvesting are determined. The model uses three trophic levels to represent the behavior of the food web system, which consists of small pelagic fish, Nile tilapia, and Nile perch. This section defines the variables, parameters, and assumptions used in the study. This is followed by a compartmental diagram that illustrates the food chain interaction among the three fish species. Lastly, the formulation of the state system and cost functional is presented.

#### 4.2.1 Definitions of variables and parameters

The fish species population is divided into classes (state variables) as follows:

- $N_1(t)$ : The biomass of small pelagic fish at any time  $t$
- $N_2(t)$ : The biomass of Nile tilapia at any time  $t$
- $N_3(t)$ : The biomass of Nile perch at any time  $t$

Each species  $N_i$ ,  $i = 1, 2, 3$ , is harvested at a rate  $h_i(t)$ , which serves as a control variable. The parameters relating to the interaction between species, growth, and harvesting are defined as follows:

- $r_1$  : The intrinsic growth rate of small pelagic fish
- $r_2$  : The intrinsic growth rate of Nile tilapia
- $r_3$  : The intrinsic growth rate of Nile perch
- $K_1$  : The carrying capacity of small pelagic fish
- $K_2$  : The carrying capacity of Nile tilapia
- $K_3$  : The carrying capacity of Nile perch
- $n_{32}$ : The growth rate of Nile perch due to predation of Nile tilapia
- $n_{31}$ : The growth rate of Nile perch due to predation of small pelagic fish
- $n_{21}$ : The growth rate of Nile tilapia due to predation of small pelagic fish
- $n_{23}$ : The consumption rate of Nile tilapia due to its predator Nile perch
- $n_{13}$ : The consumption rate of small pelagic fish due to its predator Nile perch
- $n_{12}$ : The consumption rate of small pelagic fish due to its predator Nile tilapia

## 4.2.2 Model assumptions

The following assumptions were used in the formulation of the model.

- (i) Nile perch are predators of both Nile tilapia and small pelagic fish.
- (ii) Small pelagic fish is a prey to Nile tilapia.
- (iii) The predation of Nile perch by Nile tilapia is negligible.

## 4.2.3 Compartmental diagram

The interaction between the three species,  $N_1$ ,  $N_2$ , and  $N_3$  for a food chain, is shown in Figure 4.1.

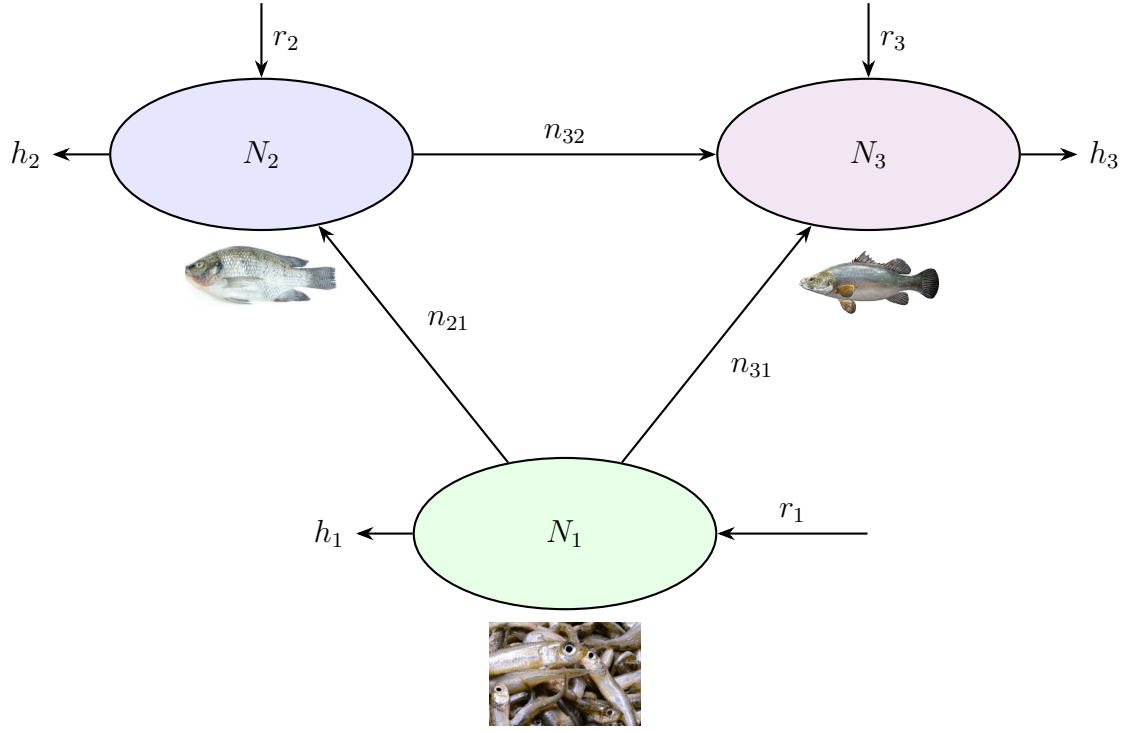


Figure 4.1: The compartmental diagram for the food chain model.

#### 4.2.4 The state equations

From the assumptions of the model and Figure 4.1, the ODE system is formulated:

$$\begin{cases} \frac{dN_1}{dt} = r_1 N_1 \left(1 - \frac{N_1}{K_1}\right) - n_{13} N_1 N_3 - n_{12} N_1 N_2 - h_1 N_1, & N_1(0) = (N_1)_0, \\ \frac{dN_2}{dt} = r_2 N_2 \left(1 - \frac{N_2}{K_2}\right) + n_{21} N_2 N_1 - n_{23} N_2 N_3 - h_2 N_2, & N_2(0) = (N_2)_0, \\ \frac{dN_3}{dt} = r_3 N_3 \left(1 - \frac{N_3}{K_3}\right) + n_{32} N_3 N_2 + n_{31} N_3 N_1 - h_3 N_3, & N_3(0) = (N_3)_0. \end{cases} \quad (4.1)$$

Note that  $n_{12} N_1 N_2$ ,  $n_{13} N_1 N_3$ , and  $n_{23} N_2 N_3$  are the decay terms, while  $n_{21} N_2 N_1$ ,  $n_{31} N_3 N_1$ , and  $n_{32} N_3 N_2$  are the growth terms resulting from the predator-prey interaction between different fish species. The terms,  $r_1 N_1 \left(1 - \frac{N_1}{K_1}\right)$ ,  $r_2 N_2 \left(1 - \frac{N_2}{K_2}\right)$ , and  $r_3 N_3 \left(1 - \frac{N_3}{K_3}\right)$  represent the logistics growth terms of  $N_1$ ,  $N_2$ , and  $N_3$ , respectively, as a result of intra-specific competition. Throughout this work, the right-hand side of the problem (4.1) is denoted by the function  $g(t, N)$ .

Additionally,  $N_i(t)$ ,  $i = 1, 2, 3$  are the state variables that belong to the space of continuously differentiable functions over the finite time interval  $[0, T]$ . This guarantees a

well-defined and smooth dynamics of the fish population:

$$N_i(t) \in C^1([0, T]) \mid 0 < N_i(t) \leq B_i, \quad i = 1, 2, 3.$$

The symbol  $B_i$  represents the positive constants representing the maximum feasible population limits for the different species of fish. The system of equations (4.1) admits unique solutions (see Theorem 7). However, a criterion needs to be established to identify the optimal solutions, that is, the solutions that maximise the net profit from fishing. Thus, a criterion is defined in the form of a cost functional  $J(h_1, h_2, h_3)$ .

**Definition 3.** *The cost functional  $J$  is defined as the total revenue minus the cost of fishing:*

$$J(h_1, h_2, h_3) = \int_0^T \sum_{i=1}^3 ((p_i h_i N_i - c_i h_i - \mu_i h_i^2 N_i^2) dt. \quad (4.2)$$

Here,  $J(h_1, h_2, h_3)$  represents the net profit of fishing. The term  $p_i h_i N_i$  is the revenue with unit price  $p_i$ , while  $(c_i h_i + \mu_i h_i^2 N_i^2)$  denotes the cost, where  $c_i > 0$  and  $\mu_i > 0$  are the coefficients of the linear and quadratic cost terms, respectively, where  $i = 1, 2, 3$ .

The aim of Definition 3 is to specify the optimal controls  $h_i^*$  in  $\mathcal{A}$  that maximise the cost functional (4.2) provided that

$$J(h_1^*, h_2^*, h_3^*) = \max_{(h_1, h_2, h_3) \in \mathcal{A}} J(h_1, h_2, h_3).$$

The symbol  $\mathcal{A}$  is a class of admissible controls represented by

$$\mathcal{A} = \left\{ h(t) = (h_1(t), h_2(t), h_3(t)) : [0, T] \rightarrow \mathbb{R}^3 \left| \begin{array}{l} h_i \text{ is Lebesgue measurable, } 0 \leq h_i(t) \leq M_i, \\ M_i \in \mathbb{R}_{\geq 0}, \text{ and } i = 1, 2, 3 \end{array} \right. \right\}. \quad (4.3)$$

### 4.3 Existence and Uniqueness of State Solutions

Here, the focus is on proving the existence and uniqueness of the solutions for the state system (4.1).

**Theorem 6** (Peano's Existence Theorem). *If the function  $g(t, N)$  is continuous in a neighborhood of  $t = 0$ , where  $N = (N_1, N_2, N_3)^T$ , then the initial value problem (4.1) has at least one solution defined in a neighborhood of  $t = 0$ .*

See [Pouso \(2012\)](#) for a comprehensive and accessible modern proof of [Theorem 6](#), along with several important refinements.

**Theorem 7** (Lipschitz Uniqueness Theorem). *Let the function  $g(t, N)$  be continuous for all  $(t, N) \in E$ . If  $g(t, N)$  satisfies the Lipschitz condition in [Lemma 2](#), then the initial value problem [\(4.1\)](#) admits a unique solution in a neighborhood of  $t = 0$ .*

From [Lemma 2](#) it follows that  $g(t, N)$  satisfies the Lipschitz condition, which implies that the initial value problem [\(4.1\)](#) admits a unique solution in a neighborhood of  $t = 0$  ([Agarwal & O'Regan, 2008](#), pg. 68). Based on [Theorem 6](#) and [Theorem 7](#), there exists a unique state solution.

## 4.4 Existence and Uniqueness of the Optimal Controls

In this section, the existence of a unique optimal control  $h_i^*(t)$ ,  $i = 1, 2, 3$  is shown for the optimal control problem [\(4.1\)](#)-[\(4.2\)](#).

**Theorem 8.** *Suppose  $(N_i^*(t), h_i^*(t))$ ,  $i = 1, 2, 3$ , is an admissible pair. If the admissible control set  $\mathcal{A}$  is convex and the cost functional  $J(h_1, h_2, h_3)$  is strictly concave in  $(h_1, h_2, h_3)$ , then there exists a unique optimal control  $(h_1^*, h_2^*, h_3^*) \in \mathcal{A}$  such that*

$$J(h_1^*, h_2^*, h_3^*) = \max_{(h_1, h_2, h_3) \in \mathcal{A}} J(h_1, h_2, h_3).$$

Using the same approach as in [Section 3.4](#), [Theorem 8](#) is proved. However, the strict concavity of the cost functional  $J$ , in [Definition 3](#), for  $h_i(t)$  and  $N_i(t)$  is due to the quadratic term  $-\mu_i h_i^2 N_i^2$ , where  $-\mu_i < 0$  ([Lenhart & Workman, 2007](#), pg. 26). Hence, a unique optimal control exists within a class of admissible control [\(4.3\)](#).

## 4.5 Positivity and Boundedness of the State Solutions

In this section, the positivity of the state solutions is proven, and subsequently, they are shown to be uniformly bounded.

**Theorem 9.** *If  $N_1(t)$ ,  $N_2(t)$ , and  $N_3(t)$ , are the solutions of the state system [\(4.1\)](#), then there exist constants  $B_1, B_2, B_3 > 0$  provided*

$$0 < N_1(t) \leq B_1, \quad 0 < N_2(t) \leq B_2, \quad 0 < N_3(t) \leq B_3, \quad \forall t \in [0, T].$$

Applying the same procedures as in Section 3.5, Theorem 9 is proved. This ensures that the fish population stays above zero and grows within a biologically feasible limit, due to resource and space limitations.

## 4.6 The Optimality System

Here, Pontryagin's maximum principle is used to formulate the optimality system, comprising the state system, the adjoint equations, and the optimality condition (Pontryagin et al., 1967). The Hamiltonian  $\mathcal{H}$  is derived by incorporating the state equations (4.1) and the cost functional (4.2).

**Definition 4.** *The Hamiltonian  $\mathcal{H}$  is defined as*

$$\begin{aligned} \mathcal{H} = & (p_1 h_1 N_1 - c_1 h_1 - \mu_1 h_1^2 N_1^2) + (p_2 h_2 N_2 - c_2 h_2 - \mu_2 h_2^2 N_2^2) \\ & + (p_3 h_3 N_3 - c_3 h_3 - \mu_3 h_3^2 N_3^2) \\ & + \lambda_1 \left( r_1 N_1 \left( 1 - \frac{N_1}{K_1} \right) - n_{13} N_1 N_3 - n_{12} N_1 N_2 - h_1 N_1 \right) \\ & + \lambda_2 \left( r_2 N_2 \left( 1 - \frac{N_2}{K_2} \right) + n_{21} N_2 N_1 - n_{23} N_2 N_3 - h_2 N_2 \right) \\ & + \lambda_3 \left( r_3 N_3 \left( 1 - \frac{N_3}{K_3} \right) + n_{32} N_3 N_2 + n_{31} N_3 N_1 - h_3 N_3 \right). \end{aligned} \quad (4.4)$$

The symbols  $\lambda_1(t)$ ,  $\lambda_2(t)$ , and  $\lambda_3(t)$  are the adjoint variables associated with their respective states  $N_1(t)$ ,  $N_2(t)$ , and  $N_3(t)$ .

### 4.6.1 Adjoint equations

The existence of the adjoint function is obtained using Pontryagin's maximum principle. The adjoint equations are derived using the Hamiltonian (4.4) as follows (Lenhart & Workman, 2007).

$$\frac{d\lambda_1}{dt} = -\frac{\partial \mathcal{H}}{\partial N_1}, \quad \frac{d\lambda_2}{dt} = -\frac{\partial \mathcal{H}}{\partial N_2}, \quad \frac{d\lambda_3}{dt} = -\frac{\partial \mathcal{H}}{\partial N_3}.$$

This results in the following.

$$\begin{aligned}
\frac{d\lambda_1}{dt} &= - \left[ p_1 h_1 - 2\mu_1 h_1^2 N_1 + \lambda_1 \left( r_1 \left( 1 - \frac{2N_1}{K_1} \right) - n_{13} N_3 - n_{12} N_2 - h_1 \right) + \lambda_2 n_{21} N_2 + \lambda_3 n_{31} N_3 \right], \\
\frac{d\lambda_2}{dt} &= - \left[ p_2 h_2 - 2\mu_2 h_2^2 N_2 - \lambda_1 n_{12} N_1 + \lambda_2 \left( r_2 \left( 1 - \frac{2N_2}{K_2} \right) + n_{21} N_1 - n_{23} N_3 - h_2 \right) + \lambda_3 n_{32} N_3 \right], \\
\frac{d\lambda_3}{dt} &= - \left[ p_3 h_3 - 2\mu_3 h_3^2 N_3 - \lambda_1 n_{13} N_1 - \lambda_2 n_{23} N_2 + \lambda_3 \left( r_3 \left( 1 - \frac{2N_3}{K_3} \right) + n_{32} N_2 + n_{31} N_1 - h_3 \right) \right], \\
\lambda_i(T) &= 0, \quad i = 1, 2, 3.
\end{aligned} \tag{4.5}$$

## 4.6.2 Optimality condition

The optimality condition is obtained by differentiating the Hamiltonian  $\mathcal{H}$ , in Definition 4 partially with respect to the control variables  $h_1$ ,  $h_2$ , and  $h_3$ :

$$\begin{cases} \frac{\partial \mathcal{H}}{\partial h_1} = p_1 N_1 - c_1 - 2\mu_1 h_1 N_1^2 - \lambda_1 N_1, \\ \frac{\partial \mathcal{H}}{\partial h_2} = p_2 N_2 - c_2 - 2\mu_2 h_2 N_2^2 - \lambda_2 N_2, \\ \frac{\partial \mathcal{H}}{\partial h_3} = p_3 N_3 - c_3 - 2\mu_3 h_3 N_3^2 - \lambda_3 N_3. \end{cases} \tag{4.6}$$

Differentiating the first, second, and third equations in (4.6) with respect to the controls  $h_1$ ,  $h_2$ , and  $h_3$ , respectively, yields the following.

$$\begin{aligned}
\frac{\partial^2 \mathcal{H}}{\partial h_1^2} &= -2\mu_1 N_1^2, \\
\frac{\partial^2 \mathcal{H}}{\partial h_2^2} &= -2\mu_2 N_2^2, \\
\frac{\partial^2 \mathcal{H}}{\partial h_3^2} &= -2\mu_3 N_3^2.
\end{aligned}$$

Since  $\mu_i > 0$  and  $N_i^2 > 0$ ,  $i = 1, 2, 3$ , then

$$\frac{\partial^2 \mathcal{H}}{\partial h_1^2} < 0, \quad \frac{\partial^2 \mathcal{H}}{\partial h_2^2} < 0, \quad \frac{\partial^2 \mathcal{H}}{\partial h_3^2} < 0.$$

Hence, a maximisation optimal control problem. Three distinct cases for characterising the optimal controls  $h_i^*$ ,  $i = 1, 2, 3$ , were considered as follows:

$$h_i^*(t) = \begin{cases} 0 & ; \quad \frac{\partial \mathcal{H}}{\partial h_i} < 0, \\ 0 \leq h_i^*(t) \leq M_i & ; \quad \frac{\partial \mathcal{H}}{\partial h_i} = 0, \\ M_i & ; \quad \frac{\partial \mathcal{H}}{\partial h_i} > 0, \end{cases} \quad (4.7)$$

where  $i = 1, 2, 3$ . Next, each of the three cases is considered as follows.

Case 1. Using  $\frac{\partial \mathcal{H}}{\partial h_i} = 0$ ,  $i = 1, 2, 3$  in (4.6), yields

$$\begin{cases} \frac{\partial \mathcal{H}}{\partial h_1} = p_1 N_1 - c_1 - 2\mu_1 h_1 N_1^2 - \lambda_1 N_1 = 0, \\ \frac{\partial \mathcal{H}}{\partial h_2} = p_2 N_2 - c_2 - 2\mu_2 h_2 N_2^2 - \lambda_2 N_2 = 0, \\ \frac{\partial \mathcal{H}}{\partial h_3} = p_3 N_3 - c_3 - 2\mu_3 h_3 N_3^2 - \lambda_3 N_3 = 0. \end{cases} \quad (4.8)$$

Solving for  $h_1$ ,  $h_2$ , and  $h_3$  in (4.8), yields the optimal harvest rates  $h_1^*$ ,  $h_2^*$ , and  $h_3^*$ , respectively.

$$\begin{aligned} h_1^* &= \frac{(p_1 - \lambda_1)N_1 - c_1}{2\mu_1 N_1^2}, \\ h_2^* &= \frac{(p_2 - \lambda_2)N_2 - c_2}{2\mu_2 N_2^2}, \\ h_3^* &= \frac{(p_3 - \lambda_3)N_3 - c_3}{2\mu_3 N_3^2}. \end{aligned}$$

Using the conditions in (4.7), it implies

$$\begin{cases} 0 \leq h_1^*(t) = \frac{(p_1 - \lambda_1)N_1 - c_1}{2\mu_1 N_1^2} \leq M_1, & t \in [0, T], \\ 0 \leq h_2^*(t) = \frac{(p_2 - \lambda_2)N_2 - c_2}{2\mu_2 N_2^2} \leq M_2, & t \in [0, T], \\ 0 \leq h_3^*(t) = \frac{(p_3 - \lambda_3)N_3 - c_3}{2\mu_3 N_3^2} \leq M_3, & t \in [0, T]. \end{cases} \quad (4.9)$$

Case 2. Using  $\frac{\partial \mathcal{H}}{\partial h_1} < 0$ ,  $\frac{\partial \mathcal{H}}{\partial h_2} < 0$ , and  $\frac{\partial \mathcal{H}}{\partial h_3} < 0$  with  $h_1^* = h_2^* = h_3^* = 0$  in (4.6), gives

$$\begin{cases} \frac{\partial \mathcal{H}}{\partial h_1} = p_1 N_1 - c_1 - \lambda_1 N_1 < 0, \\ \frac{\partial \mathcal{H}}{\partial h_2} = p_2 N_2 - c_2 - \lambda_2 N_2 < 0, \\ \frac{\partial \mathcal{H}}{\partial h_3} = p_3 N_3 - c_3 - \lambda_3 N_3 < 0. \end{cases} \quad (4.10)$$

Since  $\mu_i > 0$  and  $N_i^2 > 0$  for each  $i = 1, 2, 3$ , (4.10) reduces to

$$\begin{aligned}\frac{(p_1 - \lambda_1)N_1 - c_1}{2\mu_1 N_1^2} &< 0 = h_1(t), \quad t \in [0, T], \\ \frac{(p_2 - \lambda_2)N_2 - c_2}{2\mu_2 N_2^2} &< 0 = h_2(t), \quad t \in [0, T], \\ \frac{(p_3 - \lambda_3)N_3 - c_3}{2\mu_3 N_3^2} &< 0 = h_3(t), \quad t \in [0, T].\end{aligned}$$

Thus,

$$\begin{cases} h_1^*(t) = \max\left(0, \frac{(p_1 - \lambda_1^*)N_1^* - c_1}{2\mu_1 (N_1^*)^2}\right), & t \in [0, T], \\ h_2^*(t) = \max\left(0, \frac{(p_2 - \lambda_2^*)N_2^* - c_2}{2\mu_2 (N_2^*)^2}\right), & t \in [0, T], \\ h_3^*(t) = \max\left(0, \frac{(p_3 - \lambda_3^*)N_3^* - c_3}{2\mu_3 (N_3^*)^2}\right), & t \in [0, T]. \end{cases} \quad (4.11)$$

Case 3. Using  $\frac{\partial \mathcal{H}}{\partial h_1} > 0$ ,  $\frac{\partial \mathcal{H}}{\partial h_2} > 0$ , and  $\frac{\partial \mathcal{H}}{\partial h_3} > 0$  with  $h_1^* = M_1$ ,  $h_2^* = M_2$ , and  $h_3^* = M_3$  in (4.6), gives

$$\begin{cases} p_1 N_1 - c_1 - 2\mu_1 M_1 N_1^2 - \lambda_1 N_1 > 0, & t \in [0, T], \\ p_2 N_2 - c_2 - 2\mu_2 M_2 N_2^2 - \lambda_2 N_2 > 0, & t \in [0, T], \\ p_3 N_3 - c_3 - 2\mu_3 M_3 N_3^2 - \lambda_3 N_3 > 0, & t \in [0, T]. \end{cases} \quad (4.12)$$

Since  $\mu_i > 0$  and  $N_i^2 > 0$  for each  $i = 1, 2, 3$ , (4.12) is simplified as:

$$\begin{aligned}\frac{(p_1 - \lambda_1)N_1 - c_1}{2\mu_1 N_1^2} &> M_1 = h_1(t), \quad t \in [0, T], \\ \frac{(p_2 - \lambda_2)N_2 - c_2}{2\mu_2 N_2^2} &> M_2 = h_2^*(t), \quad t \in [0, T], \\ \frac{(p_3 - \lambda_3)N_3 - c_3}{2\mu_3 N_3^2} &> M_3 = h_3^*(t), \quad t \in [0, T].\end{aligned}$$

Therefore:

$$\begin{cases} h_1^*(t) = \min\left(M_1, \frac{(p_1 - \lambda_1^*)N_1^* - c_1}{2\mu_1 (N_1^*)^2}\right), & t \in [0, T], \\ h_2^*(t) = \min\left(M_2, \frac{(p_2 - \lambda_2^*)N_2^* - c_2}{2\mu_2 (N_2^*)^2}\right), & t \in [0, T], \\ h_3^*(t) = \min\left(M_3, \frac{(p_3 - \lambda_3^*)N_3^* - c_3}{2\mu_3 (N_3^*)^2}\right), & t \in [0, T]. \end{cases} \quad (4.13)$$

In view of the three cases (4.9), (4.11), and (4.13), the optimality condition is obtained

as

$$\begin{cases} h_1^*(t) = \min \left( M_1, \max \left( 0, \frac{(p_1 - \lambda_1^*)N_1^* - c_1}{2\mu_1(N_1^*)^2} \right) \right), & t \in [0, T], \\ h_2^*(t) = \min \left( M_2, \max \left( 0, \frac{(p_2 - \lambda_2^*)N_2^* - c_2}{2\mu_2(N_2^*)^2} \right) \right), & t \in [0, T], \\ h_3^*(t) = \min \left( M_3, \max \left( 0, \frac{(p_3 - \lambda_3^*)N_3^* - c_3}{2\mu_3(N_3^*)^2} \right) \right), & t \in [0, T]. \end{cases} \quad (4.14)$$

The optimality system comprises the state system (4.1), the adjoint equations (4.5), and the optimality condition (4.14).

## 4.7 Parameter Estimation

Adopting the parameter values estimated in Section 3.7, with the exception of cost coefficients. The linear cost coefficient in Table 3.1 represents the cost per unit quantity of fish harvested. However, in the constant effort harvesting model, the linear cost coefficient  $c_i, i = 1, 2, 3$  represents the cost per unit harvest rate  $h_i$ , where the harvested quantity is given by  $h_i N_i, i = 1, 2, 3$ , in (4.2). The values of  $c_i$  in Table 4.1 represent the product of the cost per unit of harvest and the estimated fish biomass, later scaled to cost per unit tonne of harvest rate. Table 4.1 summarises all the parameters and their sources.

Table 4.1: Parameter descriptions and values under constant effort harvesting strategies.

Parameter	Description	Value	Source
$r_1$	Intrinsic growth rate of $N_1$	0.6546	Mpele et al. (2014b)
$r_2$	Intrinsic growth rate of $N_2$	0.1112	Mpele et al. (2014b)
$r_3$	Intrinsic growth rate of $N_3$	0.4770	Mpele et al. (2014b)
$n_{32}$	Growth rate of $N_3$ due to predation of $N_2$	0.004	Estimated
$n_{23}$	Consumption rate of $N_2$ due to its predator $N_3$	0.004	Estimated
$n_{31}$	Growth rate of $N_3$ due to predation of $N_1$	0.005	Mpele et al. (2014a)
$n_{13}$	Consumption rate of $N_1$ due to its predator $N_3$	0.005	Mpele et al. (2014a)
$n_{21}$	Growth rate of $N_2$ due to predation of $N_1$	0.005	Mpele et al. (2014a)
$n_{12}$	Consumption rate of $N_1$ due to its predator $N_2$	0.005	Mpele et al. (2014a)
$K_1$	Carrying capacity of $N_1$	38.24 tons	Estimated
$K_2$	Carrying capacity of $N_2$	3.54 tons	Estimated
$K_3$	Carrying capacity of $N_3$	9.36 tons	Estimated
$p_1$	Price per unit biomass of $N_1$	US\$ $22.7 \times 10^6$	Estimated
$p_2$	Price per unit biomass of $N_2$	US\$ $24.0 \times 10^6$	Estimated
$p_3$	Price per unit biomass of $N_3$	US\$ $200 \times 10^6$	Estimated
$c_1$	Linear cost coefficient for $N_1$	US\$ $713.0 \times 10^6$	Estimated
$c_2$	Linear cost coefficient for $N_2$	US\$ $166.0 \times 10^6$	Estimated
$c_3$	Linear cost coefficient for $N_3$	US\$ $2560 \times 10^6$	Estimated
$\mu_1$	Quadratic cost coefficient for $N_1$	US\$ $1 \times 10^5$	Estimated
$\mu_2$	Quadratic cost coefficient for $N_2$	US\$ $2 \times 10^5$	Estimated
$\mu_3$	Quadratic cost coefficient for $N_3$	US\$ $4 \times 10^5$	Estimated

## 4.8 Numerical Simulations

The model was formulated using nonlinear ODEs (4.1) subject to constant effort harvesting for the three fish species. The cost functional (4.2) in Definition 3 played a key role in maximising the net profit of fishing for the three species by balancing harvesting benefits against the associated costs. Additionally, the existence and uniqueness of the optimal solutions were proven. Furthermore, the positivity and boundedness of the state solutions were proven. The derivation of the optimality system was performed using the PMP, and it was subsequently solved using the forward-backward sweep method, implemented with the fourth-order Runge-Kutta scheme; detailed MATLAB code is provided in Appendix C.

### 4.8.1 Optimal solutions

Implementing the forward-backward sweep with parameter values in Table 4.1, the optimal solutions obtained are presented in Figure 4.2 and Table 4.2. In Figure 4.2(a), the result indicates that the highest optimal harvest rate is recorded for Nile perch, followed by Nile tilapia, and the least optimal harvest rate is recorded for small pelagic fish. The highest optimal harvest rate leads to a reduction in the predation pressure on species at lower trophic levels, thereby contributing to the balance of the ecosystem. The low optimal harvest rates for  $N_1$  and  $N_2$  are to ensure that the prey are not extinct.

The population dynamics of three fish species depicted in Figure 4.2(b) show that the biomass of small pelagic fish ( $N_1$ ) increases rapidly due to low initial biomass compared to its carrying capacity and high intrinsic growth rate. The optimal biomass is reached below the carrying capacity as a result of harvest and predation from  $N_2$  and  $N_3$ . For Nile tilapia ( $N_2$ ), the biomass decreases because of its low intrinsic growth rate, high initial biomass compared to its carrying capacity, and vulnerability to predation. However, the optimal biomass is attained above the carrying capacity as a result of a low optimal harvest rate. The population of Nile perch ( $N_3$ ) first decreases slightly as a result of intra-species competition. The biomass increases towards the optimal level due to its predatory role, leading to the optimal biomass being higher than the carrying capacity.

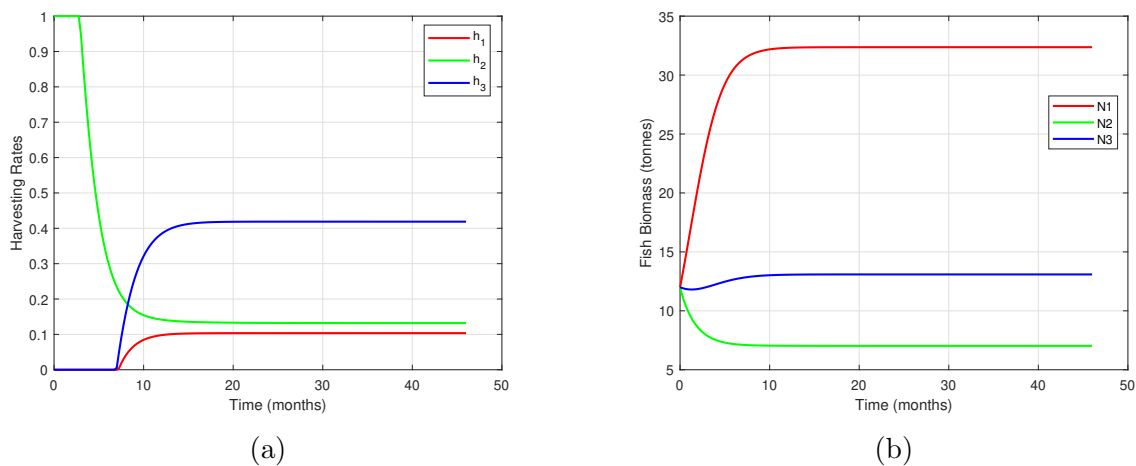


Figure 4.2: (a) Optimal harvest rate and (b) Biomass of small pelagic fish, Nile tilapia, and Nile perch under constant effort harvesting strategies.

The summary of optimal solutions for the model (4.1)-(4.2) is presented in Table 4.2.

Table 4.2: Summary of the results for the optimal solutions under constant effort harvesting strategies.

Optimal solution	Fish species	Optimal value
Harvest Rate	Small pelagic fish, $h_1^*$	0.10356
	Nile tilapia, $h_2^*$	0.13200
	Nile perch, $h_3^*$	0.41879
Fish Biomass	Small pelagic fish, $N_1^*$	32.36551 tonnes
	Nile tilapia, $N_2^*$	7.02524 tonnes
	Nile perch, $N_3^*$	13.08690 tonnes

#### 4.8.2 Dynamics of fish populations with different harvest rates

The effects of varying harvest rates on each fish population dynamics are illustrated in Figure 4.3, for three different harvest levels. In particular, the population dynamics for optimal harvest rates  $h_i^*$ ,  $i = 1, 2, 3$  obtained from Table 4.2, were compared with reduced harvest rates  $0.5h_i^*$  (below optimal), and increased harvest rates  $1.5h_i^*$  (above optimal). Figure 4.3 shows that fish biomass for all the species decreases as harvest rates increase and vice versa. When harvest rates are reduced below optimal levels, the biomass settles at a higher level compared to optimal biomass for the three fish species, indicating enhanced ecological conservation but potentially reduced economic returns. In contrast, exceeding optimal harvest rates causes a significant reduction in fish biomass across the three species, reflecting overexploitation and potential long-term ecological harm. For optimal harvest rates, it stabilises at a point that enhances both ecological sustainability and long-term economic return.

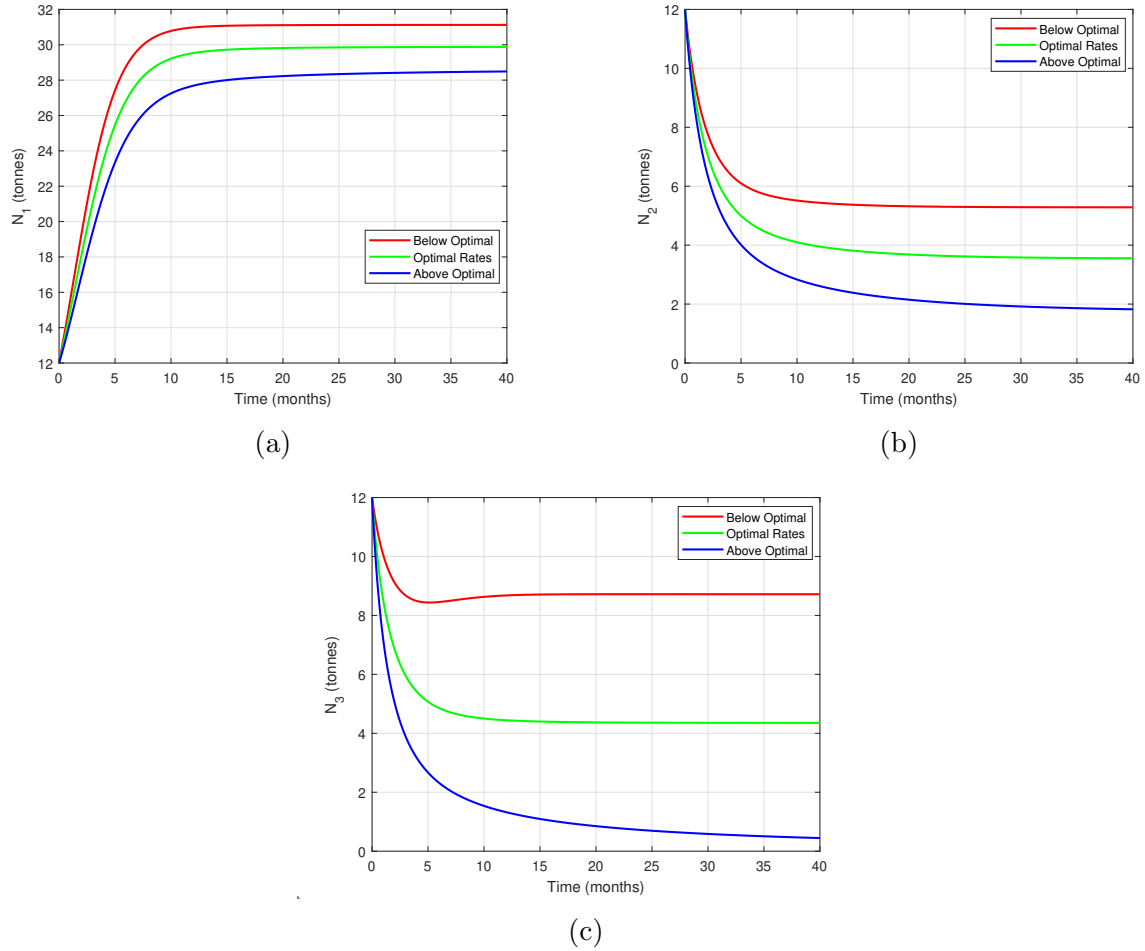
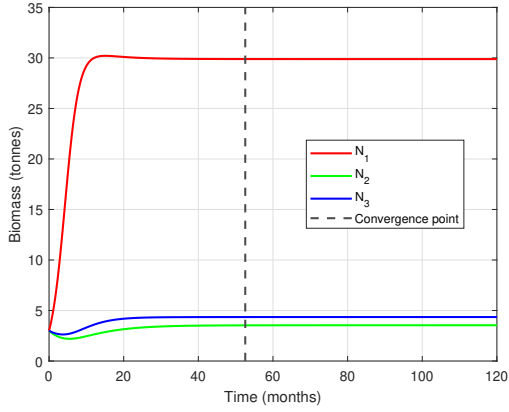


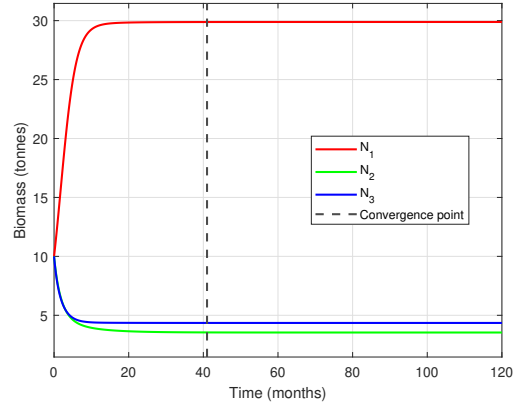
Figure 4.3: Variation of fish populations with time for different harvest rates: (a) small pelagic fish, (b) Nile tilapia, (c) Nile perch

### 4.8.3 The influence of different initial biomass on the dynamics of fish populations

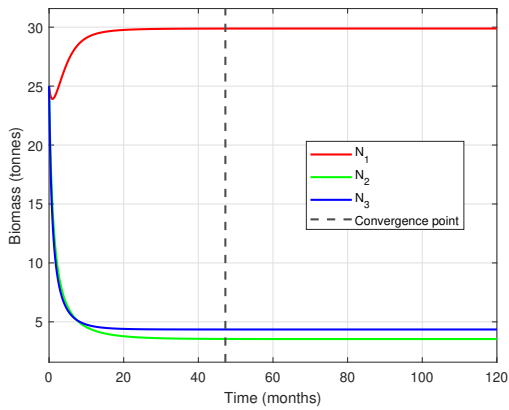
The influence of varying initial biomass on the dynamics of each fish population at optimal harvest rates is presented, as illustrated in Figure 4.4. Figure 4.4 shows that the initial biomass does not influence the optimal values but significantly affects the simulation time to attain the optimal level, since the harvest depends on the available biomass. Figure 4.4(a) reveals that at low initial biomass, the fish population requires a relatively longer simulation time, which reduces with an increase in initial biomass, as shown in Figure 4.4(b) and (c). For high initial biomass, the fish population requires a relatively longer simulation time, as illustrated in Figure 4.4(d). The least simulation time is recorded for moderate initial biomass as shown in Figure 4.4(b). Balancing the initial biomass also increases the simulation time as illustrated in Figure 4.4(d) and (e). This is due to intraspecific competition for the few available prey.



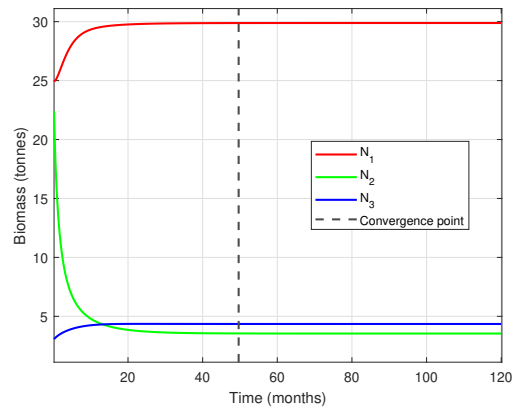
(a)  $(N_1)_0 = 3$ ,  $(N_2)_0 = 3$ , and  $(N_3)_0 = 3$



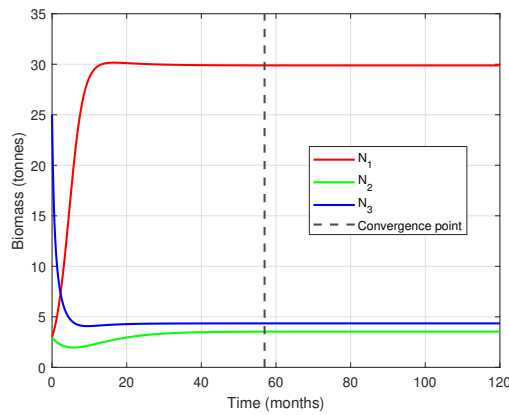
(b)  $(N_1)_0 = 10$ ,  $(N_2)_0 = 10$ , and  $(N_3)_0 = 10$



(c)  $(N_1)_0 = 25$ ,  $(N_2)_0 = 25$ , and  $(N_3)_0 = 25$



(d)  $(N_1)_0 = 25$ ,  $(N_2)_0 = 25$ , and  $(N_3)_0 = 3$



(e)  $(N_1)_0 = 3$ ,  $(N_2)_0 = 3$ , and  $(N_3)_0 = 25$

Figure 4.4: Variation of fish populations with time for different initial conditions ( $2 \leq (N_i)_0 \leq 30$   $i = 1, 2, 3$ )

# Chapter 5

## Discussions, Conclusions, and Recommendations

### 5.1 Introduction

A comprehensive discussion of the results obtained in Chapters 3 and 4 is presented, concerning the different optimal harvesting strategies at Lake Albert, Uganda. In this chapter, further conclusions and recommendations are provided to support sustainable fishing practices.

### 5.2 Discussions

The study investigated the population dynamics of three key fish species: small pelagic fish, Nile tilapia, and Nile perch. The models were developed using nonlinear ordinary differential equations to represent the biological interactions and responses of the species under constant yield and constant effort harvesting strategies. The optimal control problem was theoretically analysed, proving the existence, uniqueness, positivity, and boundedness of the state solutions, together with the existence and uniqueness of the optimal controls. Furthermore, Pontryagin's maximum principle was used to derive the optimality system, while the forward-backward sweep method was used to approximate the optimal solutions.

The population dynamics of three fish species under constant effort harvesting reveal a distinct pattern. Small pelagic fish exhibit rapid biomass growth and stabilise at a higher optimal biomass, due to their high logistic growth, despite being below the carrying capacity as a result of harvest and predation. The population of Nile tilapia decreases because of its low intrinsic growth rate and vulnerability to predation, which leads to the lowest optimal biomass. Interestingly, the biomass of Nile perch stabilises above its

carrying capacity as a result of its predatory role. The corresponding optimal harvesting rates, determined iteratively using the FBS method, indicate that Nile perch has the highest optimal harvest rate due to its dominance and potential predators for other species. Small pelagic fish have the lowest optimal harvest rate, preserving their essential role as prey in the ecosystem.

Under constant yield harvesting, the simulation results showed that the harvest rates for the fish species remain steady throughout the two-year period, which aligns with its definition in (Alfred, 2016; Idels & Wang, 2008). The highest harvest rate is recorded for Nile perch, leading to a reduction in predation pressure on other species at lower trophic levels. The lowest rate for Nile tilapia ensures that the prey does not go to extinction. The moderate optimal harvest for small pelagic fish is to maintain a relatively high species biomass, since it is a prey in the ecosystem. The fish population dynamic under constant yield harvesting reveals that the biomass of small pelagic fish increases rapidly but stabilises below their carrying capacity due to predation and harvest. Nile tilapia biomass decreases but stabilises above its carrying capacity due to a low optimal harvest rate. Finally, Nile perch biomass stabilises at a lower level compared to its carrying capacity due to intra-species competition and a high optimal harvest rate. These population dynamics highlight the complex interspecies interactions and the trade-offs involved in getting the optimal harvest rates.

Furthermore, the results highlight clear trends in fish population when harvest rates are varied. For constant effort harvesting, reducing harvest rates below optimal levels results in an increase in biomass for the three fish species, indicating enhanced biological conservation but potentially reduced economic returns. However, increasing harvesting rates beyond the optimal level causes significant reductions in fish biomass, reflecting overexploitation and potential long-term ecological harm. This result is consistent with the finding of Mpele et al. (2014a), who considered optimal taxation strategies in a three-species fishery system in Lake Victoria. Similarly, under constant yield harvesting, harvesting below the optimal level supports higher species biomass, preserving ecological balance but possibly reducing economic return. In contrast, exceeding optimal harvest rates leads to even more drastic consequences, including the extinction of the Nile perch. This result is in agreement with that of Alfred (2016); Laham et al. (2012), where constant yield harvesting does not give time for the fish population to recover if the harvest is above the equilibrium point.

Varying initial biomass highlights its critical role in the fish population dynamics. For constant yield harvesting, the impact of initial biomass is more severe. Low initial biomass exposes a higher risk of extinction of fish species due to competition for limited resources.

Under moderate initial biomass, faster fish population recovery is supported, while high biomass requires longer simulation time to reach the optimal level due to high interspecific competition and harvest. Under constant effort harvesting, initial biomass does not influence the optimal values but significantly affects the simulation time to attain the optimal level. Low and high initial biomass result in prolonged recovery, while moderate initial biomass leads to shorter convergence time.

### 5.3 Conclusions

In this work, a cost functional that maximises the net profit from fishing was formulated and analysed over a finite time horizon. It accounted for economic gains from harvesting three key fish species: small pelagic fish, Nile tilapia, and Nile perch in Lake Albert, Uganda. The models incorporated constant effort and constant yield harvesting strategies to determine the optimal harvesting strategies. The dynamics of the fish population were governed by a system of nonlinear ODEs that represent logistic growth, predation between species, and the harvesting terms. An optimality system was derived using Pontryagin's maximum principle, yielding state equations, adjoint equations, and optimality conditions. To approximate the optimal system, a forward-backward sweep method was implemented using the fourth-order Runge-Kutta scheme.

In the model with constant yield harvesting, the optimal harvesting strategy for fish populations was obtained by determining the optimal harvest rates and the corresponding optimal biomass. The optimal harvest rates determined were constant throughout the simulation period, regardless of the fish biomass. The highest optimal harvest rate is recorded for Nile perch, resulting in reduced predation pressure on other species, contributing to the balance of the ecosystem. Small pelagic fish have a low optimal harvest rate that reflects their role as prey in the ecosystem and supports its ecological resilience. The lowest optimal harvest rate was recorded for Nile tilapia to prevent species extinction, due to a low intrinsic growth rate and vulnerability to predation. The impact of varying initial biomass influences the population dynamics. Low initial biomass increases the risk of extinction for fish species due to competition for limited resources. The moderate initial biomass supports faster fish population recovery, while high biomass requires longer simulation time to reach the optimal level due to high intraspecific competition and harvest.

The optimal conditions for the co-existence of fish populations under a constant effort harvesting model were ascertained by determining the optimal solutions and getting initial conditions that prevent slow recovery or extinction of fish species. The highest optimal

harvest rate is recorded for Nile perch, followed by Nile tilapia, and the lowest observed for small pelagic fish. The highest optimal harvest rate leads to a reduction in the predation pressure on species at lower trophic levels, thereby enhancing ecosystem balance. The low optimal harvest rates for small pelagic fish and Nile tilapia are to safeguard prey populations from extinction. While initial biomass does not alter the optimal values under this strategy, it significantly influences the simulation time to attain the optimal level. Low and high initial biomass result in prolonged recovery, while moderate initial biomass leads to shorter convergence time. The findings underscore the importance of applying optimal harvesting and maintaining moderate biomass levels as the key strategies for the co-existence of all fish species in the ecosystem.

The optimal harvesting strategies for fish population using both constant yield and constant effort harvesting were established through the determination of the optimal solutions and initial conditions that achieve the optimal values. When comparing the two harvesting strategies, constant effort harvesting is more effective and sustainable compared to constant yield harvesting, since its harvest rates are dependent on the available biomass, thereby preventing overexploitation when the fish populations are low. Although initial biomass affects the recovery time, the flexibility of the optimal harvest ensures population recovery without driving the population to extinction. In contrast, constant yield harvesting applies a fixed harvest rate that is independent of the fish biomass. This poses a high risk of slow species recovery and extinction at low initial biomass. The results indicate that constant yield harvesting is highly sensitive to over-exploitation compared to constant effort harvesting strategies.

## 5.4 Recommendations

Based on the findings, optimal harvesting strategies are recommended, as they promote ecological sustainability by preventing both overexploitation and underutilisation of resources, thus improving ecological balance and economic efficiency. In a scenario where fish populations go below thresholds, the implementation of precautionary no-take zones is recommended to avoid irreversible stock collapse. Further studies that incorporate more fish species and interspecific interactions are recommended to guide the generalisation of the optimal harvesting strategies to the entire Lake Albert ecosystem, considering the complexity of its fish populations.

Lastly, future work should extend the current model to incorporate spatial-temporal dynamics to better capture the heterogeneous distribution and movement patterns of fish species across different zones of the lake. Additionally, the model did not consider the migration of the three fish species. One should include the migration of the species to have a more realistic model.

# References

- Action, S. I. (2020). World fisheries and aquaculture. *Food and Agriculture Organisation, 2020*, 1-244.
- Agarwal, R. P., & O'Regan, D. (2008). *An introduction to ordinary differential equations*. New York: Springer.
- Alfred, D. A. C. I. (2016). Fish Harvesting Models and Their Applications in a Reservoir in Saranda, Albania. *Journal of Multidisciplinary Engineering Science and Technology*, 3(7), 5279-5282.
- Anița, S., Arnautu, V., & Capasso, V. (2011). *An introduction to optimal control problems in life sciences and economics: From mathematical models to numerical simulation with MATLAB®*. Springer Science & Business Media.
- Béné, C., Barange, M., Subasinghe, R., Pinstруп-Andersen, P., Merino, G., Hemre, G. I., & Williams, M. (2015). Feeding 9 billion by 2050—Putting fish back on the menu. *Food Security*, 7, 261-274.
- Brilliant Uganda. (2025). *Lakes of Uganda*. Brilliant Uganda. Retrieved April 27, 2025, from <https://www.brilliant-uganda.com/lakes-of-uganda>
- Chaudhuri, K. (1986). A bioeconomic model of harvesting a multispecies fishery. *Ecological Modelling*, 32(4), 267–279. [https://doi:10.1016/0304-3800\(86\)90091-8](https://doi:10.1016/0304-3800(86)90091-8)
- Chen, P., & Islam, S. M. (2005). *Optimal control models in finance: a new computational approach*. Boston, MA: Springer US.
- Clark, C. W. (1990). *Mathematical Bioeconomics: the Optimal Management of Renewable Resources*. Pure and applied mathematics (John Wiley and Sons: Unnumbered). Wiley, New York, 2nd ed. edition.
- Clark, C. W., & Munro, G. R. (1975). The economics of fishing and modern capital theory: A simplified approach. *Journal of Environmental Economics and Management*, 2(2), 92–106. [https://doi:10.1016/0095-0696\(75\)90002-9](https://doi:10.1016/0095-0696(75)90002-9).

- Da Rocha, J. M., Gutiérrez, M. J., & Cerviño, S. (2012). Reference points based on dynamic optimisation: a versatile algorithm for mixed-fishery management with bio-economic age-structured models. *ICES Journal of Marine Science*, 69(4), 660-669.
- Demir, M., & Lenhart, S. (2019). Optimal sustainable fishery management of the Black Sea anchovy with food chain modelling framework. *Natural Resource Modelling*, <https://doi:10.1111/nrm.12253>.
- Hannachi, A., & Hossain, M. (2017). Numerical methods for optimal control problems in fisheries management. *Mathematical Modelling and Analysis*, 22 (3), 337-355.
- Idels, L. V., & Wang, M. (2008). Harvesting fisheries management strategies with modified effort function. *International Journal of Modelling, Identification and Control*, 3(1), 83. <https://doi:10.1504/ijmic.2008.018188>.
- Kellner, J. R., & Sweeney, A. (2016). Challenges in data-driven decision making in fisheries management: The role of data quality and uncertainty. *Fisheries Research*, 182, 1-12.
- Khamis, S. A., Tchuenche, J. M., Lukka, M., & Heiliö, M. (2011). Dynamics of fisheries with prey reserve and harvesting. *International Journal of Computer Mathematics*, 88(8), 1776–1802. <https://doi:10.1080/00207160.2010.527001>.
- La Torre, D., Kunze, H., Ruiz-Galan, M., Malik, T., & Marsiglio, S. (2015). Optimal control: theory and application to science, engineering, and social sciences. In *Abstract and applied analysis* (Vol. 2015). John Wiley & Sons, Inc..
- Laham, M. F., Krishnarajah, I. S., & Shariff, J. M. (2012). Fish harvesting management strategies using logistic growth model. *Sains Malaysiana*, 41(2), 171-177.
- Lenhart, S., & Workman, J. T. (2007). *Optimal Control Applied to Biological Models*. Chapman and Hall/CRC, Boca Raton.
- Maurya, A., & Priyadarshi, A. (2020). Fish harvesting strategies with Allee effect. *ITM Web of Conferences*, 34, 02004. <https://doi.org/10.1051/itmconf/20203402004>.
- McDougall, C. (2023). *Illuminating Hidden Harvests: the contributions of small-scale fisheries to sustainable development*.
- Meyer, C. D. (2023). *Matrix analysis and applied linear algebra*. Society for Industrial and Applied Mathematics.
- Mpele, J. P., Nkansah-Gyekye, Y., & Makinde, O. D. (2014). A dynamic model for a three species open-access fishery with taxation as a control instrument of harvesting efforts the case of Lake Victoria. *Commun. Math. Biol. Neurosci.*, 2014.

- Mpele, J. P., Nkansah-Gyekye, Y., & Makinde, O. D. (2014). Estimating sustainable harvests of Lake Victoria fishery. *International Journal of Applied Mathematics*, 27(4), 407–416. <https://doi.org/10.12732/ijam.v27i4.7>
- Namukonge, S., & Barakagira, A. (2024). Viability and Profitability of Cage Fish Farming on Lake Victoria: *A Case of Bugiri-Kiwuulwe Cage Fish Farms in Wakiso District, Uganda*.
- Pontryagin, L. S., Boltyanskii, V. G., Gamkrelidze, R. V., & Mishchenko, E. F. (1962). The mathematical theory of optimal processes, translated by KN Trirogoff. New York.
- Pontryagin, L. S., Boltyanskii, V. G., Gamkrelidze, R. V., & Mishchenko, E. F. (1967). The mathematical theory of optimal processes. *Wiley, New York*.
- Pouso, R. L. (2012). Peano’s Existence Theorem revisited. *arXiv e-prints*, arXiv-1202.
- Raymond, C., Hugo, A., & Kungaro, M. (2019). Modelling Dynamics of Prey-Predator Fishery Model with Harvesting: *A Bioeconomic Model*. *Journal of Applied Mathematics*, 2019, 1–13. <https://doi:10.1155/2019/2601648>
- Rossi, S. (2022). Fishing and Overfishing-Sustainable Harvest of the Sea. In *SDG 14: Life Below Water: A Machine-Generated Overview of Recent Literature* (pp. 207-325). Cham: Springer International Publishing.
- Sahoo, B., & Poria, S. (2015). Effects of Allochthonous Resources in a Three Species Food Chain Model with Harvesting. *Differential Equations and Dynamical Systems*, 23(3), 257–279. <https://doi:10.1007/s12591-014-0209-7>
- Seijo, J. C., Defeo, O., & Salas, S. (1998). *Fisheries bioeconomics. Theory, modelling and management*.
- Selina Wamucii. (2025). *Nile perch prices in Uganda*. Selina Wamucii. <https://www.selinawamucii.com/insights/prices/uganda/Nile-perch/>
- Selina Wamucii. (2025). *Tilapia prices in Uganda*. Selina Wamucii. <https://www.selinawamucii.com/insights/prices/uganda/tilapia/>
- Uganda Bureau of Statistics. (2024, September). *Consumer Price Index (CPI)*. Press Release – September 2024. <https://www.ubos.org/wp-content/uploads/publications/CPI-Press-Release-September-2024.pdf>
- Wilen, J. E. (2000). Renewable resource economists and policy: what differences have we made?. *Journal of Environmental Economics and Management*, 39(3), 306-327.

# Appendices

## Appendix A: Definition

**Definition 5.** Let  $A = (a_{ij})$  be a  $3 \times 3$  matrix. The matrix norms induced by the vector 1-norm, denoted by  $\|A\|_1$ , is the maximum absolute column sum given by:

$$\|A\|_1 = \max_{1 \leq j \leq 3} \sum_{i=1}^3 |a_{ij}|.$$

Additionally, for two vectors  $x = (x_1, x_2, x_3)^T$  and  $y = (y_1, y_2, y_3)^T$  in  $\mathbb{R}^3$ , the Euclidean norm (2-norm) of their difference is the measure of the Euclidean distance between the vectors  $x$  and  $y$ , is defined by:

$$\|x - y\|_2 = \left( \sum_{i=1}^3 (x_i - y_i)^2 \right)^{1/2}$$

(Meyer, 2023).

## Appendix B: MATLAB codes for solving the model under constant yield harvesting

```

1 clc; clear; close all;
2 %% Time settings
3 T = 118;           % Final time
4 dt = 0.25;        % Time step
5 N = round(T/dt);  % Number of time steps
6 t = linspace(0, T, N+1); % Time discretisation
7 % Parameters
8 r1 = 0.6546; K1 = 38.24; n12 = 0.005; n13 = 0.005; p1 = 22.7e6;
   c1 = 10e6; mu1 = 4e6; M1 = 5;
9 r2 = 0.1112; K2 = 3.54; n21 = 0.005; n23 = 0.004; p2 = 24e6;
   c2 = 19e6; mu2 = 7e6; M2 = 5;
10 r3 = 0.4770; K3 = 9.36; n31 = 0.005; n32 = 0.004; p3 = 200e6;
   c3 = 150e6; mu3 = 14e6; M3 = 5;
11 % Initial and transversality conditions
12 N1 = zeros(1, N+1); N1(1) = 12;
13 N2 = zeros(1, N+1); N2(1) = 12;
14 N3 = zeros(1, N+1); N3(1) = 12;
15
16 h1 = 1 * ones(1, N+1);
17 h2 = 1 * ones(1, N+1);
18 h3 = 1 * ones(1, N+1);
19
20 lambda1 = zeros(1, N+1); lambda1(end) = 0;
21 lambda2 = zeros(1, N+1); lambda2(end) = 0;
22 lambda3 = zeros(1, N+1); lambda3(end) = 0;
23 % Iteration limits
24 max_iter = 100;
25 tol = 1e-6;
26
27 for iter = 1:max_iter
28     % Keep the previous controls for convergence check
29     h1_old = h1; h2_old = h2; h3_old = h3;
30     % Forward sweep (state equations)
31     for i = 1:N
32         S1 = @(N1,N2,N3,h1) r1*N1*(1 - N1/K1) - n13*N1*N3 - n12*
           N1*N2 - h1;

```

```

33     S2 = @(N1,N2,N3,h2) r2*N2*(1 - N2/K2) + n21*N2*N1 - n23*
        N2*N3 - h2;
34     S3 = @(N1,N2,N3,h3) r3*N3*(1 - N3/K3) + n32*N3*N2 + n31*
        N3*N1 - h3;
35
36     k1_1 = S1(N1(i), N2(i), N3(i), h1(i));
37     k1_2 = S2(N1(i), N2(i), N3(i), h2(i));
38     k1_3 = S3(N1(i), N2(i), N3(i), h3(i));
39
40     k2_1 = S1(N1(i)+0.5*dt*k1_1, N2(i)+0.5*dt*k1_2, N3(i)
        +0.5*dt*k1_3, 0.5*(h1(i)+h1(i+1)));
41     k2_2 = S2(N1(i)+0.5*dt*k1_1, N2(i)+0.5*dt*k1_2, N3(i)
        +0.5*dt*k1_3, 0.5*(h2(i)+h2(i+1)));
42     k2_3 = S3(N1(i)+0.5*dt*k1_1, N2(i)+0.5*dt*k1_2, N3(i)
        +0.5*dt*k1_3, 0.5*(h3(i)+h3(i+1)));
43
44     k3_1 = S1(N1(i)+0.5*dt*k2_1, N2(i)+0.5*dt*k2_2, N3(i)
        +0.5*dt*k2_3, 0.5*(h1(i)+h1(i+1)));
45     k3_2 = S2(N1(i)+0.5*dt*k2_1, N2(i)+0.5*dt*k2_2, N3(i)
        +0.5*dt*k2_3, 0.5*(h2(i)+h2(i+1)));
46     k3_3 = S3(N1(i)+0.5*dt*k2_1, N2(i)+0.5*dt*k2_2, N3(i)
        +0.5*dt*k2_3, 0.5*(h3(i)+h3(i+1)));
47
48     k4_1 = S1(N1(i)+dt*k3_1, N2(i)+dt*k3_2, N3(i)+dt*k3_3, h1
        (i+1));
49     k4_2 = S2(N1(i)+dt*k3_1, N2(i)+dt*k3_2, N3(i)+dt*k3_3, h2
        (i+1));
50     k4_3 = S3(N1(i)+dt*k3_1, N2(i)+dt*k3_2, N3(i)+dt*k3_3, h3
        (i+1));
51
52     N1(i+1) = N1(i) + dt*(k1_1 + 2*k2_1 + 2*k3_1 + k4_1)/6;
53     N2(i+1) = N2(i) + dt*(k1_2 + 2*k2_2 + 2*k3_2 + k4_2)/6;
54     N3(i+1) = N3(i) + dt*(k1_3 + 2*k2_3 + 2*k3_3 + k4_3)/6;
55     end
56     % Backward sweep (adjoint equations)
57     for i = N:-1:1
58         A1 = @(l1,l2,l3,n1,n2,n3) -(l1*(r1*(1 - 2*n1/K1) - n12*n2
        - n13*n3) + l2*n21*n2 + l3*n31*n3);
59
60         A2 = @(l1,l2,l3,n1,n2,n3) -(-l1*n12*n1 + l2*(r2*(1 - 2*n2
        /K2) + n21*n1 - n23*n3) + l3*n32*n3);

```

```

61
62 A3 = @(l1,l2,l3,n1,n2,n3) -(-l1*n13*n1 - l2*n23*n2 + l3*(
        r3*(1 - 2*n3/K3) + n32*n2 + n31*n1));
63
64 k1_1 = A1(lambda1(i+1), lambda2(i+1), lambda3(i+1), N1(i
        +1), N2(i+1), N3(i+1));
65 k1_2 = A2(lambda1(i+1), lambda2(i+1), lambda3(i+1), N1(i
        +1), N2(i+1), N3(i+1));
66 k1_3 = A3(lambda1(i+1), lambda2(i+1), lambda3(i+1), N1(i
        +1), N2(i+1), N3(i+1));
67
68 k2_1 = A1(lambda1(i+1)-0.5*dt*k1_1, lambda2(i+1)-0.5*dt*
        k1_2, lambda3(i+1)-0.5*dt*k1_3, 0.5*(N1(i)+N1(i+1)),
        0.5*(N2(i)+N2(i+1)), 0.5*(N3(i)+N3(i+1)));
69 k2_2 = A2(lambda1(i+1)-0.5*dt*k1_1, lambda2(i+1)-0.5*dt*
        k1_2, lambda3(i+1)-0.5*dt*k1_3, 0.5*(N1(i)+N1(i+1)),
        0.5*(N2(i)+N2(i+1)), 0.5*(N3(i)+N3(i+1)));
70 k2_3 = A3(lambda1(i+1)-0.5*dt*k1_1, lambda2(i+1)-0.5*dt*
        k1_2, lambda3(i+1)-0.5*dt*k1_3, 0.5*(N1(i)+N1(i+1)),
        0.5*(N2(i)+N2(i+1)), 0.5*(N3(i)+N3(i+1)));
71
72 k3_1 = A1(lambda1(i+1)-0.5*dt*k2_1, lambda2(i+1)-0.5*dt*
        k2_2, lambda3(i+1)-0.5*dt*k2_3, 0.5*(N1(i)+N1(i+1)),
        0.5*(N2(i)+N2(i+1)), 0.5*(N3(i)+N3(i+1)));
73 k3_2 = A2(lambda1(i+1)-0.5*dt*k2_1, lambda2(i+1)-0.5*dt*
        k2_2, lambda3(i+1)-0.5*dt*k2_3, 0.5*(N1(i)+N1(i+1)),
        0.5*(N2(i)+N2(i+1)), 0.5*(N3(i)+N3(i+1)));
74 k3_3 = A3(lambda1(i+1)-0.5*dt*k2_1, lambda2(i+1)-0.5*dt*
        k2_2, lambda3(i+1)-0.5*dt*k2_3, 0.5*(N1(i)+N1(i+1)),
        0.5*(N2(i)+N2(i+1)), 0.5*(N3(i)+N3(i+1)));
75
76 k4_1 = A1(lambda1(i+1)-dt*k3_1, lambda2(i+1)-dt*k3_2,
        lambda3(i+1)-dt*k3_3, N1(i), N2(i), N3(i));
77 k4_2 = A2(lambda1(i+1)-dt*k3_1, lambda2(i+1)-dt*k3_2,
        lambda3(i+1)-dt*k3_3, N1(i), N2(i), N3(i));
78 k4_3 = A3(lambda1(i+1)-dt*k3_1, lambda2(i+1)-dt*k3_2,
        lambda3(i+1)-dt*k3_3, N1(i), N2(i), N3(i));
79
80 lambda1(i) = lambda1(i+1) - dt*(k1_1 + 2*k2_1 + 2*k3_1 +
        k4_1)/6;

```

```

81     lambda2(i) = lambda2(i+1) - dt*(k1_2 + 2*k2_2 + 2*k3_2 +
      k4_2)/6;
82     lambda3(i) = lambda3(i+1) - dt*(k1_3 + 2*k2_3 + 2*k3_3 +
      k4_3)/6;
83     end
84     % Update controls
85     h1 = min(M1, max(0, 0.5 * (h1_old + (p1 - lambda1 - c1)./(2*
      mu1)))));
86     h2 = min(M2, max(0, 0.5 * (h2_old + (p2 - lambda2 - c2)./(2*
      mu2)))));
87     h3 = min(M3, max(0, 0.5 * (h3_old + (p3 - lambda3 - c3)./(2*
      mu3)))));
88     % Convergence check
89     err = max([max(abs(h1 - h1_old)), max(abs(h2 - h2_old)), max(
      abs(h3 - h3_old))]);
90     if err < tol
91         converged = true;
92         fprintf('Converged at iteration %d with error %.2e\n',
      iter, err);
93         break;
94     end
95 end
96 % Final results
97 fprintf('\nFinal values at T = %.2f:\n', T);
98 fprintf('h1(T) = %.5f, h2(T) = %.5f, h3(T) = %.5f\n', h1(end), h2
      (end), h3(end));
99 fprintf('N1(T) = %.5f, N2(T) = %.5f, N3(T) = %.5f\n', N1(end), N2
      (end), N3(end));
100 % For smooth plots of the state and control variables
101 t_fine = linspace(0, T, 10*N);
102
103 N1_smooth = interp1(t, N1, t_fine, 'spline');
104 N2_smooth = interp1(t, N2, t_fine, 'spline');
105 N3_smooth = interp1(t, N3, t_fine, 'spline');
106
107 h1_smooth = interp1(t, h1, t_fine, 'spline');
108 h2_smooth = interp1(t, h2, t_fine, 'spline');
109 h3_smooth = interp1(t, h3, t_fine, 'spline');
110
111 % The plots for State and Control Variables (Optimal solutions)
112 figure;

```

```
113 plot(t_fine, N1_smooth, 'r', t_fine, N2_smooth, 'g', t_fine,
      N3_smooth, 'b', 'LineWidth', 1.5);
114 xlabel('Time (months)'); ylabel('Fish Biomass (tonnes)');
115 title('');
116 legend('N1', 'N2', 'N3'); grid on; legend('Location', 'best');
117
118 figure;
119 plot(t_fine, h1_smooth, 'r', t_fine, h2_smooth, 'g', t_fine,
      h3_smooth, 'b', 'LineWidth', 1.5);
120 xlabel('Time (months)'); ylabel('Harvest Rates');
121 title('');
122 legend('h1', 'h2', 'h3'); grid on; legend('Location', 'best');
```

## Appendix C: MATLAB codes for solving the model under constant effort harvesting

```

1 clc; clear; close all;
2 % Time settings
3 T = 46;           % Final time
4 dt = 0.25;       % Time step
5 N = round(T/dt); % Number of time steps
6 t = linspace(0, T, N+1); % Time discretisation
7 % Parameters
8 r1 = 0.6546; K1 = 38.24; n12 = 0.005; n13 = 0.005; p1 = 22.7e6;
   c1 = 713e6; mu1 = 0.1e6; M1 = 1;
9 r2 = 0.1112; K2 = 3.54; n21 = 0.005; n23 = 0.004; p2 = 24e6;
   c2 = 166e6; mu2 = 0.2e6; M2 = 1;
10 r3 = 0.4770; K3 = 9.36; n31 = 0.005; n32 = 0.004; p3 = 200e6;
   c3 = 2560e6; mu3 = 0.4e6; M3 = 1;
11 % Initial and transversality conditions
12 N1 = zeros(1, N+1); N1(1) = 12;
13 N2 = zeros(1, N+1); N2(1) = 12;
14 N3 = zeros(1, N+1); N3(1) = 12;
15
16 h1 = 0.5 * ones(1, N+1);
17 h2 = 0.5 * ones(1, N+1);
18 h3 = 0.5 * ones(1, N+1);
19
20 lambda1 = zeros(1, N+1); lambda1(end) = 0;
21 lambda2 = zeros(1, N+1); lambda2(end) = 0;
22 lambda3 = zeros(1, N+1); lambda3(end) = 0;
23 % Iteration limits
24 max_iter = 100;
25 tol = 1e-6;
26
27 for iter = 1:max_iter
28 % Keep the previous controls for convergence check
29     h1_old = h1; h2_old = h2; h3_old = h3;
30 % Forward sweep for solving state equations
31     for i = 1:N
32         S1 = @(N1,N2,N3,h1) r1*N1*(1 - N1/K1) - n13*N1*N3 - n12*N1*
           N2 - h1*N1;

```

```

33 S2 = @(N1,N2,N3,h2) r2*N2*(1 - N2/K2) + n21*N2*N1 - n23*N2*
N3 - h2*N2;
34 S3 = @(N1,N2,N3,h3) r3*N3*(1 - N3/K3) + n32*N3*N2 + n31*N3*
N1 - h3*N3;
35
36 k1_1 = S1(N1(i), N2(i), N3(i), h1(i));
37 k1_2 = S2(N1(i), N2(i), N3(i), h2(i));
38 k1_3 = S3(N1(i), N2(i), N3(i), h3(i));
39
40 k2_1 = S1(N1(i)+0.5*dt*k1_1, N2(i)+0.5*dt*k1_2, N3(i)
+0.5*dt*k1_3, 0.5*(h1(i)+h1(i+1)));
41 k2_2 = S2(N1(i)+0.5*dt*k1_1, N2(i)+0.5*dt*k1_2, N3(i)
+0.5*dt*k1_3, 0.5*(h2(i)+h2(i+1)));
42 k2_3 = S3(N1(i)+0.5*dt*k1_1, N2(i)+0.5*dt*k1_2, N3(i)
+0.5*dt*k1_3, 0.5*(h3(i)+h3(i+1)));
43
44 k3_1 = S1(N1(i)+0.5*dt*k2_1, N2(i)+0.5*dt*k2_2, N3(i)
+0.5*dt*k2_3, 0.5*(h1(i)+h1(i+1)));
45 k3_2 = S2(N1(i)+0.5*dt*k2_1, N2(i)+0.5*dt*k2_2, N3(i)
+0.5*dt*k2_3, 0.5*(h2(i)+h2(i+1)));
46 k3_3 = S3(N1(i)+0.5*dt*k2_1, N2(i)+0.5*dt*k2_2, N3(i)
+0.5*dt*k2_3, 0.5*(h3(i)+h3(i+1)));
47
48 k4_1 = S1(N1(i)+dt*k3_1, N2(i)+dt*k3_2, N3(i)+dt*k3_3, h1
(i+1));
49 k4_2 = S2(N1(i)+dt*k3_1, N2(i)+dt*k3_2, N3(i)+dt*k3_3, h2
(i+1));
50 k4_3 = S3(N1(i)+dt*k3_1, N2(i)+dt*k3_2, N3(i)+dt*k3_3, h3
(i+1));
51
52 N1(i+1) = N1(i) + dt*(k1_1 + 2*k2_1 + 2*k3_1 + k4_1)/6;
53 N2(i+1) = N2(i) + dt*(k1_2 + 2*k2_2 + 2*k3_2 + k4_2)/6;
54 N3(i+1) = N3(i) + dt*(k1_3 + 2*k2_3 + 2*k3_3 + k4_3)/6;
55 end
56 % Backward sweep for solving adjoint equations
57 for i = N:-1:1
58 A1 = @(l1,l2,l3,n1,n2,n3,h1) -(p1*h1 - 2*mu1*h1^2*n1 + l1*(r1
*(1 - 2*n1/K1) - n13*n3 - n12*n2 - h1) + l2*n21*n2 + l3*
n31*n3);
59

```

```

60  A2 = @(l1,l2,l3,n1,n2,n3,h2) -(p2*h2 - 2*mu2*h2^2*n2 - l1*n12
    *n1 + l2*(r2*(1 - 2*n2/K2) + n21*n1 - n23*n3 - h2) + l3*
    n32*n3);
61
62  A3 = @(l1,l2,l3,n1,n2,n3,h3) -(p3*h3 - 2*mu3*h3^2*n3 - l1*n13
    *n1 - l2*n23*n2 + l3*(r3*(1 - 2*n3/K3) + n32*n2 + n31*n1 -
    h3));
63
64  k1_1 = A1(lambda1(i+1), lambda2(i+1), lambda3(i+1), N1(i
    +1), N2(i+1), N3(i+1), h1(i));
65  k1_2 = A2(lambda1(i+1), lambda2(i+1), lambda3(i+1), N1(i
    +1), N2(i+1), N3(i+1), h2(i));
66  k1_3 = A3(lambda1(i+1), lambda2(i+1), lambda3(i+1), N1(i
    +1), N2(i+1), N3(i+1), h3(i));
67
68  k2_1 = A1(lambda1(i+1)-0.5*dt*k1_1, lambda2(i+1)-0.5*dt*
    k1_2, lambda3(i+1)-0.5*dt*k1_3, 0.5*(N1(i)+N1(i+1)),
    0.5*(N2(i)+N2(i+1)), 0.5*(N3(i)+N3(i+1)), h1(i));
69  k2_2 = A2(lambda1(i+1)-0.5*dt*k1_1, lambda2(i+1)-0.5*dt*
    k1_2, lambda3(i+1)-0.5*dt*k1_3, 0.5*(N1(i)+N1(i+1)),
    0.5*(N2(i)+N2(i+1)), 0.5*(N3(i)+N3(i+1)), h2(i));
70  k2_3 = A3(lambda1(i+1)-0.5*dt*k1_1, lambda2(i+1)-0.5*dt*
    k1_2, lambda3(i+1)-0.5*dt*k1_3, 0.5*(N1(i)+N1(i+1)),
    0.5*(N2(i)+N2(i+1)), 0.5*(N3(i)+N3(i+1)), h3(i));
71
72  k3_1 = A1(lambda1(i+1)-0.5*dt*k2_1, lambda2(i+1)-0.5*dt*
    k2_2, lambda3(i+1)-0.5*dt*k2_3, 0.5*(N1(i)+N1(i+1)),
    0.5*(N2(i)+N2(i+1)), 0.5*(N3(i)+N3(i+1)), h1(i));
73  k3_2 = A2(lambda1(i+1)-0.5*dt*k2_1, lambda2(i+1)-0.5*dt*
    k2_2, lambda3(i+1)-0.5*dt*k2_3, 0.5*(N1(i)+N1(i+1)),
    0.5*(N2(i)+N2(i+1)), 0.5*(N3(i)+N3(i+1)), h2(i));
74  k3_3 = A3(lambda1(i+1)-0.5*dt*k2_1, lambda2(i+1)-0.5*dt*
    k2_2, lambda3(i+1)-0.5*dt*k2_3, 0.5*(N1(i)+N1(i+1)),
    0.5*(N2(i)+N2(i+1)), 0.5*(N3(i)+N3(i+1)), h3(i));
75
76  k4_1 = A1(lambda1(i+1)-dt*k3_1, lambda2(i+1)-dt*k3_2,
    lambda3(i+1)-dt*k3_3, N1(i), N2(i), N3(i), h1(i));
77  k4_2 = A2(lambda1(i+1)-dt*k3_1, lambda2(i+1)-dt*k3_2,
    lambda3(i+1)-dt*k3_3, N1(i), N2(i), N3(i), h2(i));
78  k4_3 = A3(lambda1(i+1)-dt*k3_1, lambda2(i+1)-dt*k3_2,
    lambda3(i+1)-dt*k3_3, N1(i), N2(i), N3(i), h3(i));

```

```

79
80     lambda1(i) = lambda1(i+1) - dt*(k1_1 + 2*k2_1 + 2*k3_1 +
      k4_1)/6;
81     lambda2(i) = lambda2(i+1) - dt*(k1_2 + 2*k2_2 + 2*k3_2 +
      k4_2)/6;
82     lambda3(i) = lambda3(i+1) - dt*(k1_3 + 2*k2_3 + 2*k3_3 +
      k4_3)/6;
83     end
84 % Update controls using optimality condition
85 for i = 1:N+1
86     if N1(i) ~= 0
87         h1(i) = ((p1 - lambda1(i)) * N1(i) - c1) / (2 * mu1 * N1(
      i)^2);
88     else
89         h1(i) = 0;
90     end
91     if N2(i) ~= 0
92         h2(i) = ((p2 - lambda2(i)) * N2(i) - c2) / (2 * mu2 * N2(
      i)^2);
93     else
94         h2(i) = 0;
95     end
96     if N3(i) ~= 0
97         h3(i) = ((p3 - lambda3(i)) * N3(i) - c3) / (2 * mu3 * N3(
      i)^2);
98     else
99         h3(i) = 0;
100    end
101
102    % For boundary condition
103    h1(i) = min(M1, max(0, h1(i)));
104    h2(i) = min(M2, max(0, h2(i)));
105    h3(i) = min(M3, max(0, h3(i)));
106 end
107 % Convergence check
108     err = max([max(abs(h1 - h1_old)), ...
109               max(abs(h2 - h2_old)), ...
110               max(abs(h3 - h3_old))]);
111
112     if err < tol
113         converged = true;

```

```

114         fprintf('Converged at iteration %d with error %.2e\n',
115                 iter, err);
116     break;    % stop the loop
117 end
118 % Save current values for next iteration
119 h1_old = h1;
120 h2_old = h2;
121 h3_old = h3;
122 end
123
124 % Final results
125 fprintf('\nFinal values at T = %.2f:\n', T);
126 fprintf('h1(T) = %.5f, h2(T) = %.5f, h3(T) = %.5f\n', h1(end), h2
127         (end), h3(end));
128 fprintf('N1(T) = %.5f, N2(T) = %.5f, N3(T) = %.5f\n', N1(end), N2
129         (end), N3(end));
130 % For smooth plots of the state and control variables
131 t_fine = linspace(0, T, 10*N);
132
133 N1_smooth = interp1(t, N1, t_fine, 'spline');
134 N2_smooth = interp1(t, N2, t_fine, 'spline');
135 N3_smooth = interp1(t, N3, t_fine, 'spline');
136
137 h1_smooth = interp1(t, h1, t_fine, 'spline');
138 h2_smooth = interp1(t, h2, t_fine, 'spline');
139 h3_smooth = interp1(t, h3, t_fine, 'spline');
140
141 % To plot the State and Control Variables
142 figure;
143 plot(t_fine, N1_smooth, 'r', t_fine, N2_smooth, 'g', t_fine,
144      N3_smooth, 'b', 'LineWidth', 1.5);
145 xlabel('Time (months)'); ylabel('Fish Biomass (tonnes)');
146 title('');
147 legend('N1','N2','N3', 'Location', 'best'); grid on;
148
149 figure;
150 plot(t, max(0, min(1, h1)), 'r', 'LineWidth', 1.5); hold on;
151 plot(t, max(0, min(1, h2)), 'g', 'LineWidth', 1.5);
152 plot(t, max(0, min(1, h3)), 'b', 'LineWidth', 1.5);
153 xlabel('Time (months)');

```

```
151 ylabel('Harvesting Rates');  
152 legend('h_1','h_2','h_3','Location','best');  
153 title(''); grid on;
```